NOWOTWORY Journal of Oncology • 2004 • volume 54
Number 3• 195–218

Invited review

Inverse planning in brachytherapy from radium to high dose rate ^{192}Iridium afterloading

Michael Lahanas[1], Kostas Karouzakis[2], Stavroula Giannouli[2], Richard F. Mould[1] and Dimos Baltas[1,3]

We consider the inverse planning problem in brachytherapy, i.e. the problem to determine an optimal number of catheters, number of sources for low-dose rate brachytherapy (LDR) and the optimal dwell times for high-dose rate brachytherapy (HDR) necessary to obtain an optimal as possible dose distribution.
Starting from the 1930s, inverse planning for LDR brachytherapy used geometrically derived rules to determine the optimal placement of sources in order to achieve a uniform dose distribution of a specific level in planes, spheres and cylinders. Rules and nomograms were derived which still are widely used.
With the rapid development of 3D imaging technologies and the rapidly increasing computer power we have now entered the new era of computer-based inverse planning in brachytherapy. The inverse planning is now an optimisation process adapted to the individual geometry of the patient. New inverse planning optimisation algorithms are anatomy-based that consider the real anatomy of the tumour and the organs at risk (OAR). Computer-based inverse planning considers various effects such as stability of solutions for seed misplacements which cannot ever be solved analytically without gross simplifications.
In the last few years multiobjective (MO) inverse planning algorithms have been developed which recognise the MO optimisation problem which is inherent in inverse planning in brachytherapy. Previous methods used a trial and error method to obtain a satisfactory solution. MO optimisation replaces this trial and error process by presenting a representative set of dose distributions that can be obtained. With MO optimisation it is possible to obtain information that can be used to obtain the optimum number of catheters, their position and the optimum distribution of dwell times for HDR brachytherapy. For LDR brachytherapy also the stability of solutions due to seed migration can also be improved. A spectrum of alternative solutions is available and the treatment planner can select the solution that best satisfies the clinical constraints.
The inverse planning now can be extended to include characteristics of the radioactive sources that can be used for further improving the dose distributions that can be obtained leading to a generalized inverse planning. The computer-based inverse planning provides solutions that protect the OARs and the normal tissue better than by empirical methods.
We present computer-based inverse planning algorithms used for LDR brachytherapy and currently also for HDR brachytherapy.

Planowanie odwrócone w brachyterapii

W pracy omówiono problem odwróconego planowania w brachyterapii. Planowanie odwrócone ma na celu określenie optymalnej liczby prowadnic i źródeł promieniowania w brachyterapii niskimi mocami dawki (LDR) oraz właściwy czas pozostawania źródła promieniowania w prowadnicach (dwell time) celem uzyskania najlepszej możliwej dystrybucji dawek promieniowania w brachyterapii wysokimi mocami dawki (HDR).
Dzieje planowania odwróconego sięgają lat trzydziestych XX wieku. Początkowo polegało ono na zastosowaniu zasad geometrii celem określenia punktu, w którym należało umieścić źródło promieniowania aby uzyskać najkorzystniejszą dystrybucję dawek pomiędzy poszczególnymi wyliczonymi płaszczyznami, kulami i cylindrami. Z tamtego wczesnego okresu wywodzą się zasady postępowania i nomogramy używane do dnia dzisiejszego.

[1] Department of Medical Physics & Engineering
Strahlenklinik, Klinikum Offenbach, Germany
[2] Pi-Medical Ltd. Medical Technology,
Biomedical Engineering & Consultancies, R&D Department
Athens, Greece
[3] Department of Electrical and Computer Engineering
National Technical University of Athens

Szybki rozwój trójwymiarowych technik obrazowania przebiegający z jednoczesnym postępem w dziedzinie informatyki umożliwił komputerowe planowanie odwrócone. W chwili obecnej planowanie odwrócone to proces mający na celu optymalizację postępowania w zależności od indywidualnej geometrii poszczególnych guzów. Nowe algorytmy stosowane w planowaniu odwróconym opierają się na zasadach anatomii – tak samego guza jak i otaczających go narządów krytycznych (organs at risk – OAR). Algorytmy te uwzględniają również takie elementy jak gęstość tkanek warunkująca rozproszenie dawki, co nie mogło być w żaden sposób określone analitycznie bez zastosowania znacznych uproszczeń.
W ciągu ostatnich lat pojawiły się również wielopłaszczyznowe algorytmy planowania odwróconego (Multiobjective Inverse Planning Algorithms – MO). Uwzględniają one wiele zagadnień nierozerwalnie związanych z problemami planowania wstecznego w brachyterapii. Metody stosowane wcześniej opierały się na zasadzie prób i błędów, co prowadziło stopniowo do uzyskania najlepszego możliwego rozkładu dawek. Technika MO zastępuje powtarzaną serię prób i błędów przedstawieniem możliwych do uzyskania zakresów dystrybucji dawek. Umożliwia to z kolei określenie optymalnej liczby zastosowanych prowadnic, ich najlepszego umiejscowienia i najskuteczniejszych czasów pozostawania źródeł promieniowania w prowadnicach w brachyterapii metodą HDR. W przypadku metody LDR technika MO umożliwia określenie gęstości tkanek warunkujące rozproszenie dawek. Systemy planowania oparte na technice MO przedstawiają serie możliwych rozwiązań, jak również posiadają funkcję samodzielnego wyboru rozwiązania najbardziej odpowiedniego w danej sytuacji klinicznej.
Planowanie odwrócone może obecnie być wzbogacone o charakterystykę poszczególnych źródeł promieniowania, co z kolei prowadzi do dalszego ulepszenia dystrybucji dawek. Wreszcie komputerowo przeprowadzone planowanie odwrócone dostarcza rozwiązań umożliwiających lepszą ochronę pobliskich narządów (OAR) i tkanek niż wcześniej stosowane techniki empiryczne. W pracy przedstawione zostały algorytmy planowania odwróconego z zastosowaniem techniki komputerowej stosowane tak w brachyterapii niskimi (LDR) jak i wysokimi mocami dawek (HDR).

Key words: brachytherapy, inverse planning
Słowa kluczowe: brachyterapia, planowanie odwrócone

Introduction

The term *inverse problem* is a well known mathematical term dating at least from the 19th century [1, 2] and there are several mathematical journals devoted to this topic. What is meant in simplistic terms: first you know the ideal answer, and second you take into account any constraints and mathematically determine the optimum parameter values to provide the ideal answer. In other words you have the result and the inverse problem is to determine the cause of this result. We have to solve inverse problems in geophysical studies and medical applications where it is often desired to find out the internal unknown structure of an object using measurements performed outside the object, that is, non-invasively. This can be done *e.g.* by measuring radiation, X-ray, ultrasound etc, or acoustic waves that passes through the object. The object under study can be *e.g.* the human body, or the earth crust.

An inverse problem for conformal anatomy-based brachytherapy is the problem of the complete coverage of the PTV with a dose at least equal to the prescription dose. Simultaneously dose values above specific values should be avoided in OARs and the surrounding normal tissue (NT).

A major quantity of interest in brachytherapy is the dose $D(r)=D(x,y,z)$ at a point r in the treatment volume. The dose distribution specifies the corresponding three-dimensional non-negative scalar field

$$D: R^3 \rightarrow R^+, \mathbf{r} \rightarrow D \tag{1}$$

The dependence between energy fluence Ψ and dose distribution D, $A \cdot \Psi = D$, is given by the energy absorption per mass and energy fluence unit operator A or *energy absorption operator* which describes the local energy dissipation for a given patient anatomy.

We term the mapping process from the source distribution to the dose distribution, the *dose operator*. A dose distribution is possible if there is a source distribution which is able to generate it. This depends on which source distributions can be achieved by the catheters, source dwell positions (SDP), etc.

The *dose space* {D} defines the space of all achievable dose distributions for a given patient anatomy and consequently the set of all possible energy fluences defines the *fluence space* {Ψ}. The physical and biological characteristics of the patient anatomy and of the source are used for the calculation of the *dose function*, *i.e.* the absorbed dose as a function of the location in the body.

A physician, depending on the patient, prescribes the so called *desired dose function*. The objectives are to deliver a sufficient high dose in the cancerous tissue and to protect the surrounding normal tissue (NT) and organs at risk (OAR) from excessive radiation.

While the determination of D from Ψ, the solution of the so-called *forward problem*, is possible the *inverse problem*, *i.e.* determination of Ψ for a given D is not always possible. The forward problem is the dose calculation problem for which a unique solution exists.

Even if A can in principle be inverted, the image of $A^{-1}D$ will not be always an element of {Ψ} and it is possible that the solution is not unique. This problem can be solved analytically only for very simple cases, see Figure 1.

In reality only solutions are interesting if they have a realistic number of sources inside a realistic and if possible small number of catheters. In HDR brachy-

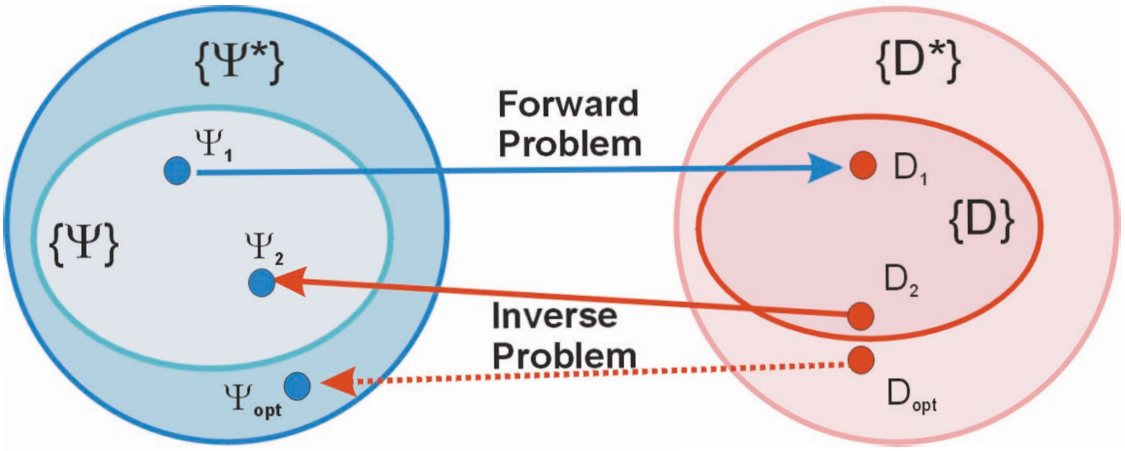

Figure 1. Forward and inverse problem in radiotherapy: The sets $\{\Psi^*\}$ and $\{D^*\}$ are all possible fluence and dose distributions respectively which include the corresponding physical possible distributions $\{\Psi\}$ and $\{D\}$. The determination of a fluence distribution from a desired optimal dose distribution D_{opt} is not always possible, such as for the two physical possible dose distributions D_1 and D_2 because the corresponding fluence distribution Ψ_{opt} may not be an element of $\{\Psi\}$

therapy, dwell positions are typically spaced up to 1 cm apart and dwell times are usually in the range of a second to a minute per dwell position. HDR procedures such as for bronchial cancer require only a single catheter and several dwell positions. Others, such as breast implants, may involve several hundred dwell positions. In interstitial breast or prostate implants some 20 catheters may be used.

As an analytical solution cannot be obtained we consider the inverse problem to determine the position and number of SDPs or sources, number of catheters and for HDR brachytherapy the dwell times, such that the obtained dose distribution satisfies as much as possible the desired dose function *via* an optimisation process. This process is called *inverse optimisation* or *inverse planning*. It includes clinical constraints such as a realistic range of catheters and the possible positions and orientations of the catheters. It is the procedure where the *ideal* implant is imaged in a virtual environment. This is based on 3D imaging which may involve CT, MR or ultrasound, and on anatomy contouring and template/catheter information. This virtual implant forms the basis for the real implant, where physicians try to work as closely as possible to obtain this virtual implant.

The determination of an optimal number of catheters is a very important aspect of inverse planning, as a reduction of the number of catheters simplifies the treatment plan in terms of time and complexity. It also reduces the possibility of treatment errors and is less invasive for the patient.

If the positions and number of catheters and the SDPs are given after the implantation of the catheters in HDR brachytherapy, we term the process *post-planning*. Then, the optimisation process to obtain an optimal dose distribution is called *dose optimisation*. Dose optimisation can be considered as a special type of inverse optimisation where the positions and number of catheters and the SDPs are fixed.

Inverse planning in brachytherapy is not a new concept and has been studied for more than 70 years. The reasons why this has only relatively recently become a topic for widespread study, is due to technological advances both in computing power (analogue computing devices were never satisfactory) and in imaging possibilities in 3D such as with CT [3-5] MR [6] and ultrasound [7] This allows very accurate localization of the prostate tumour, the OARs and the applicators [8-10].

Only currently this information is used with new dose optimisation algorithms which are termed *anatomy-based* [11-13]. The exponential growth of computing power of standard personal computers together with specialized optimisation algorithms now permits real time dose optimisation.

Only recently the multiobjective nature of dose optimisation and inverse planning has been recognized and multiobjective optimisation algorithms now provide information of the trade-off between the objectives and the limitations on the physical possible dose distributions. A spectrum of possible solutions is obtained and the treatment planner can now obtain, semi-automatically or automatically, not only a satisfactory solution but also the best solution with the least compromise on all objectives considered simultaneously. This improves the quality of the dose distributions by reducing the unnecessary dose to the smallest possible level by considering the objective functions, the anatomy and the topology of the applicators. This increases the probability of treatment success and minimizes the complication probability for the healthy surrounding tissue and the OARs.

Only seed LDR brachytherapy is considered, with radionuclides such as ^{125}I and ^{103}Pd, because the earlier methods of LDR manual afterloading of linear sources with radionuclides such as ^{226}Ra, ^{182}Ta and ^{192}Ir are no longer used. With HDR brachytherapy the source used is the single ^{192}Ir source of the remote controlled

afterloading machine which can take various dwell positions.

For LDR brachytherapy the problem is to determine the optimal position of the permanent sources (e.g. ^{125}I seeds for prostate implantation) and their number. In practice, seed sources are seldom implanted at the exact planned position due to technical difficulty and also they can move after the implantation. This misplacement obviously has a negative impact on the treatment quality. However, there is no possibility to control the LDR results unlike in HDR brachytherapy when dwell times can be modified.

We discuss only the situation where each LDR seed or HDR source dwell is inserted into catheters using a template. We term the inverse planning with this constraint *template-based inverse planning*. Template techniques are now the norm in clinical practice and therefore free-hand implants as well as being more difficult for inverse planning are not as relevant as template-based implants.

This review is divided into the topics listed in Table I.

Table I. Topics discussed in this review

Optimisation
- Optimisation objectives
- Multiobjective optimisation
- Single objective optimisation
- Decision making
- Optimisation algorithms
  - Linear and integer programming
  - Simulated annealing
  - Evolutionary algorithms
  - Multiobjective evolutionary methods

LDR brachytherapy
- The start of LDR inverse planning in the 1930s
- Current theoretical studies for LDR brachytherapy
- Strategy options for LDR brachytherapy
- Computer-based inverse planning for LDR brachytherapy
  - Iterative geometric optimisation
  - Inverse planning with simulated annealing
  - Inverse planning with evolutionary algorithms
  - Decision steered algorithm
  - Inverse planning with mixed integer programming

HDR brachytherapy
- Empirical loading methods
- Computer based methods
  - Multiobjective evolutionary inverse planning
    - Hybrid evolutionary multiobjective optimisation
    - Encoding
    - Genetic operators
- Is inverse planning for HDR brachytherapy really necessary?
- What can we learn from multiobjective inverse planning?
  - Optimal sources for optimal results

Optimisation

Optimisation objectives

An ideal dose function $D(\mathbf{r})$ with a specific prescription dose D_{ref} is:

$$\mathrm{D}(\mathbf{r}) = \begin{cases} D_{ref} \text{ if } \mathbf{r} \in \mathrm{PTV} \\ 0 \qquad \text{else} \end{cases} \tag{2}$$

This dose distribution is not obtainable since radiation can not be confined to the planning target volume (PTV) only and some part of the radiation has to traverse the OARs and the surrounding normal tissue (NT).

Out of all possible dose distributions the problem is to obtain the optimal dose distribution without any *a priori* knowledge of the physical restrictions. Optimality requires quantifying the quality of a dose distribution.

A natural measure quantifying the similarity of a dose distribution at N sampling points with dose values d_i to the corresponding optimal dose values d_i^* is a distance measure. A common measure is the L_p norm.

$$L_p = \left(\sum_{i=1}^{N} \left(d_i - d_i^* \right)^p \right)^{\frac{1}{p}} \tag{3}$$

For $p = 2$, *i.e.* L_2 we have the Euclidean distance.

The dose optimisation problem is transformed into an optimisation problem by introducing as an objective the minimization of the distance between the ideal and the achievable dose distribution. These objectives can be expressed in general by the objective functions $f_L(\mathbf{x})$ and $f_H(\mathbf{x})$

$$f_L(\mathbf{x}) = \frac{1}{N} \sum_{i=1}^{N} \Theta\left(D_L - d_i(\mathbf{x})\right)\left(D_L - d_i(\mathbf{x})\right)^p \tag{4}$$

$$f_H(\mathbf{x}) = \frac{1}{N} \sum_{i=1}^{N} \Theta\left(d_i(\mathbf{x}) - D_H\right)\left(d_i(\mathbf{x}) - D_H\right)^p \tag{5}$$

where $d_i(\mathbf{x})$ is the dose at the i$^{\text{th}}$ sampling point that depends on parameters $\mathbf{x}$ such as dwell times, p is a parameter defining the distance norm, N the number of sampling points, D_L and D_H the low and high dose limits. These are used if dose values below D_L and above D_H are to be ignored expressed by the step function $\Theta(x)$.

The difference between various dosimetric based objective functions is the norm used for defining the distance between the ideal and actual dose distribution, on how the violation is penalized and what dose normalization is applied. For $p=2$ we obtain the quadratic type of objectives [14], for $p=1$ a linear form [13]. For $p=0$ [12] the DVH-based objectives as the DVH value at the dose D_H is given by

$$DVH\left(D_H\right)=\frac{100}{N}\sum_{i=1}^{N}\Theta\left(d_i-D_H\right) \qquad (6)$$

Another method is to use dose-volume histogram (DVH) specifying constraints. These can be used for a constraint dose optimisation. Such constraints could specify upper bounds for the fraction of the volume of a region that can accept a dose larger than a specific level, or a lower bound for the fraction that should have a dose at least larger than a specific value.

Different dose distributions can be obtained if only DVH-based objectives are considered as the dose distributions are only required to satisfy some integral properties. This could be a benefit if we want to obtain a large range of possible dose distributions. It can also be a reason that various optimisation algorithms can not be used for dose optimisation.

Multiobjective optimisation

Inverse planning for brachytherapy has to consider many objectives and is thus a multiobjective (MO) problem. We have competing objectives. Increasing the dose in the PTV will increase the dose outside the PTV. A trade-off between the objectives exist and we never have a situation in which all the objectives can be in a best possible way be satisfied simultaneously.

MO optimisation provides in dose optimisation the information of all possibilities of alternative solutions we can have for a given set of objectives. By analysing the spectrum of solutions we have to decide which of these are the most appropriate according to the treatment and our clinical aims. The two steps are to solve the MO problem and decide what the optimal solution is.

The MO problem (also called multicriteria optimisation or vector optimisation), can be defined as the problem of determining the following. "A vector of decision variables which satisfies *constraints* and *optimises* a vector function whose elements represent *M* objective functions. These functions form a mathematical description of performance criteria that are usually in conflict with each other. Hence *optimises* means finding a solution which would give the values of all objective functions acceptable to the treatment planner." [15].

We call decision variables x_j, j=1,...,*N* for which values are to be chosen in an optimisation problem. For LDR brachytherapy these variables could specify which catheters and source positions should be considered. In HDR brachytherapy the dwell times have to be included in the set of decision variables.

In order to know how *good* is a certain solution, we need to have some criteria for evaluation. These criteria are expressed as computable functions $f_1(\mathbf{x}),...,f_M(\mathbf{x})$ of the decision variables, which are called *objective functions*. These form a vector function $\mathbf{f} = (f_1(\mathbf{x}),...,f_M(\mathbf{x}))$. In general, some of these will be in conflict with others, and some will have to be minimized while others are maximized. The multiobjective optimisation problem can be now defined as the problem to find the vector $\mathbf{x}=(x_1,x_2,...,x_N)$, *i.e.* solution which optimise the vector function **f**.

The constraints define the feasible region X and any point **x** in X defines a feasible solution. The vector function $\boldsymbol{f}(\mathbf{x})$ is a function that maps the set X in the set *F* that represents all possible values of the objective functions. Normally we never have a situation in which all the $f_i(\mathbf{x})$ values have an optimum in X at a common point **x**. We therefore have to establish certain criteria to determine what would be considered an *optimal* solution. One interpretation of the term optimum in multiobjective optimisation is the Pareto optimum, see Figure 2.

A solution $\mathbf{x}_1$ dominates a solution $\mathbf{x}_2$ if and only if the two following conditions are true:

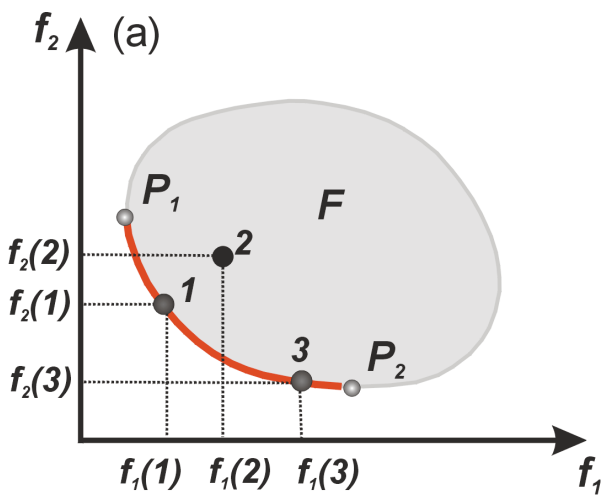

Figure 2a

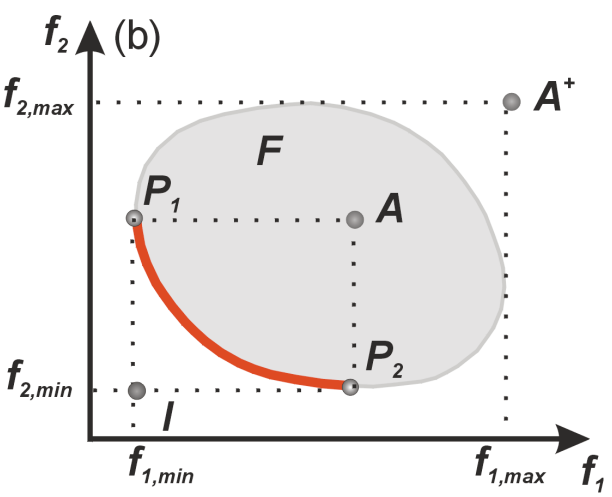

Figure 2b

Figure 2. Example of a bi-objective space (f_1, f_2). We assume a minimization problem. (a) The Pareto front is the boundary between the points P_1 and P_2 of the feasible set *F*. Solutions 1 and 3 are non-dominated Pareto optimal solutions. Solution 2 is not Pareto optimal as solution 1 has simultaneously smaller values for both objectives. There is no reason why solution 2 should be accepted rather than solution 1. Therefore the aim of MO optimisation is to obtain a representative set of non-dominated solutions. (b) The ideal and anti-ideal or nadir point *I* and *A* respectively. The point A^+ defined by Yu *et al* [16] as anti-ideal is defined over the whole *F* range, whereas the points *I* and *A* are defined by the set of efficient points

– $\mathbf{x}_1$ is no worse than $\mathbf{x}_2$ in all objectives, *i.e.* $f_j(\mathbf{x}_1) \leq f_j(\mathbf{x}_2)\ \forall$ j=1,...,*M*.
– $\mathbf{x}_1$ is strictly better than $\mathbf{x}_2$ in at least one objective, *i.e.* $f_j(\mathbf{x}_1) < f_j(\mathbf{x}_2)$ for at least one j $\in \{1,...,M\}$.

We assume, without loss of generality, that this is a minimization problem. $\mathbf{x}_1$ is said to be non-dominated by $\mathbf{x}_2$ or $\mathbf{x}_1$ is *non-inferior* to $\mathbf{x}_2$ and $\mathbf{x}_2$ is dominated by $\mathbf{x}_1$.

Among a set of solutions *P*, the non-dominated set of solutions *P'* are those that are not dominated by any other member of the set *P*, see Figure 2(a). When the set *P* is the entire feasible search space then the set *P'* is called the *global Pareto optimal set*. If for every member **x** of a set *P* there exists no solution in the neighbourhood of **x** then the solutions of *P* form a *local Pareto optimal set*. The image **f**(**x**) of the Pareto optimal set is called the *Pareto front*, see Figure 2(a). The Pareto optimal set is defined in the parameter space, while the Pareto front is defined in the objective space.

For inverse planning each solution will have a corresponding set of catheters to be selected and their number is additional to the dwell times for the SDPs of the selected catheters.

The *ideal point* and the *nadir or anti-ideal point* are characterized by the components of the best and worse objective values of efficient points respectively, see Figure 2(b).

Single objective optimisation

In single objective optimisation only one objective function is considered. Although inverse planning is a MO optimisation problem the majority of optimisation algorithms in brachytherapy are single objective optimisation algorithms. The *M* objective functions $f_m(x)$ are combined into a single objective function $f(x)$, e.g. by using a weighted sum of all objectives.

$$f(\mathbf{x}) = \sum_{m=1}^{M} w_m f_m(\mathbf{x}) \qquad (7)$$

The weights w_m are also known as *importance factors* and are considered as a measure of the significance of each objective in the optimisation process. A representative convex part of the Pareto set can be sampled by running a single objective optimisation algorithm each time with a different vector of importance factors.

We call a set of importance factors *vectors normalized and uniformly distributed* if each importance factor of each objective takes one of the following values: $[l/k, l=0,1...,k]$, where *k* is the sampling parameter and

$$\sum_{j=1}^{M} w_j = 1,\ w_j \geq 0,\ \forall j \quad \text{for each vector } \mathbf{w}.$$

For two objectives the weighted sum is given by

$$y = w_1 f_1(\mathbf{x}) + w_2 f_2(\mathbf{x}),\ i.e.\ f_2(\mathbf{x}) = -\frac{w_1}{w_2} f_1(\mathbf{x}) + \frac{y}{w_2} \qquad (8)$$

The minimization of the weighted sum can be interpreted as finding the value of *y* for which the line with slope $-w_1/w_2$ just touches the boundary of F as it proceeds outwards from the origin. If $\mathbf{x}^*$ is a Pareto optimal solution then there exists a weight vector $\mathbf{w}=(w_1,w_2,...,w_M)$, such that $\mathbf{x}^*$ is a solution of the multiobjective convex optimisation problem.

Figure 3 shows an example for a weighted sum optimisation for a bi-objective problem. The solution obtained by (w_1,w_2) is the non-dominated solution P. If the value f_1 is not satisfactory then we can increase the importance factor w_1 to w_1^*. The new set of importance factors (w_1^*,w_2) specify a new direction and the solution is P*. The value of f_1 of P* is smaller but the value f_2(P*) is larger than f_2(P). If we are not satisfied by the value of f_2(P) we can try another importance factor w_1^{**} with $w_1^* > w_1^{**} > w_1$.

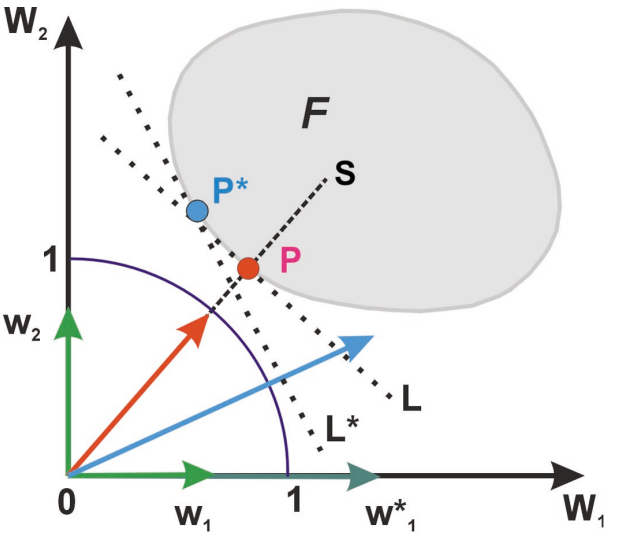

Figure 3. Single objective weighted sum optimisation $w_1f_1 + w_2f_2$ for a bi-objective problem. For a given set of importance factors the vector sum of w_1, w_2, if we consider these as vectors, specifies a direction S shown by the dashed line. The optimisation provides a solution which is the point P of a line perpendicular to the direction S that will touch the Pareto front as the line is moved away from the origin along S. Solution P* will be obtained if we replace w_1 by a larger importance factor w_1^*

In a trial and error method the optimisation is repeated with different importance factors until the treatment planner considers that the optimisation result is acceptable. The planner by a trial and error method determines the structure of the Pareto front.

While for two objectives a solution very close to the optimal can be found it is more difficult as more objectives are considered. The complexity of the Pareto front increases rapidly and also the combinatorial complexity. To determine the dependence of the results on the importance factors with a sufficient accuracy requires repeating the optimisation a large number of times with different importance factor combinations. The solution which is obtained in the conventional weighted sum approach depends on the shape of the Pareto front and the importance factors used.

Decision making

Multiobjective optimisation requires a decision making process as there is not a single solutions but a set of non-dominated solutions out of which the best must be chosen. Three strategies can be used.

- *An a priori method.* The decision making (DCM) is specified in terms of a scalar function and an optimisation engine is used to obtain the corresponding solution.
- *An a posteriori method.* An optimisation engine exists which finds a representative set of all solutions. Decision making is applied at the end of the optimisation *manually*, or using a decision engine. This method decouples the solutions from the decision making process. A new decision is possible without having to repeat the optimisation.
- *Mixture of a priori and a posteriori methods.* During the optimisation periodically information can be used which may be used to reformulate the goals as some of these can physically not be achieved.

The non-dominated solutions provide information on the trade-off between the objectives. This trade-off is described by the form of the Pareto front. In Figure 4 two different forms of trade-offs are shown.

In Figure 4(a) there is a strong trade-off between the objective f_1 and f_2. The smaller the f_1 value is that we want the larger is the corresponding f_2 value. We can see how much this depends on the choice of f_1. There is a weak trade-off between f_1 and f_2 in Figure 4(b). It is possible to minimize f_1 significant and close to the ideal point $(f_{1,\min}, f_{2,\min})$. Only very close to $f_{1,\min}$ we see a rapid increase of f_2. This is a case for a set of parameters for which we can obtain simultaneously almost the individual optimal values for f_1 and f_2. The Pareto front provides also ranges of objective values.

For more than two objectives the trade-off can be difficult to analyse graphically. A sensitivity analysis can be performed numerically such that it considers the local slope of the Pareto front as a measure of the trade-off.

The main two tasks of MO optimisation are

- Obtaining a representative set of non-dominated solutions.
- Selecting a solution from this set, i.e. the decision making process.

For MO optimisation decision-making tools are necessary to filter a single solution from the non-dominated set that matches at best the goals of the treatment planner.

DCM tools have been developed for the Real-Time HDR prostate planning system SWIFT™ (Nucletron B.V., Veenendaal, The Netherlands). A display table of a list of values for all solutions of the objectives, COIN, DVHs for all OARs, the NT and the PTV of each solution is provided. Other parameters are D_{90} (dose that covers 90% of the PTV), V_{150} (percentage of the PTV that receives more than 150% of the prescription dose).

Additionally, the extreme dose values are also provided. The entire table for every such quantity can then be sorted and solutions can be selected and highlighted by the treatment planner. Constraints can then be applied such as to show only solutions with a PTV coverage value $100c_1$ larger than a specified value. The PTV coverage is the percentage of the PTV that receives at least 100% of the prescription dose. Solutions that do not satisfy the constraints are removed from the list. This reduces the number of solutions and simplifies the selection of an optimal solution.

The DVHs of all selected solutions can be displayed and compared, see Figure 5.

Other decision-making tool could be the display of projections of the Pareto front onto a pair of selected objectives. For M objectives the number of such projections is $M(M–1)/2$.

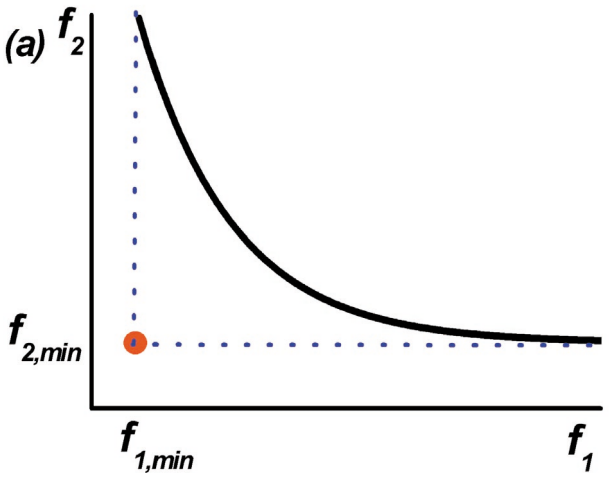

Figure 4a

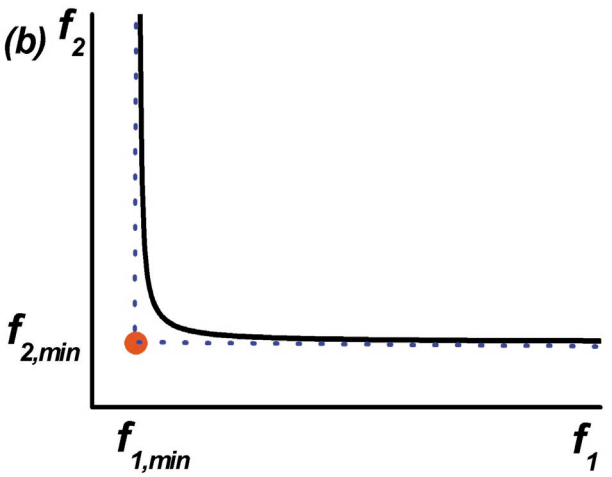

Figure 4b

Figure 4. Trade-off between two objectives of a bi-objective problem: (a) Strong and (b) weak trade-off between f_1 and f_2

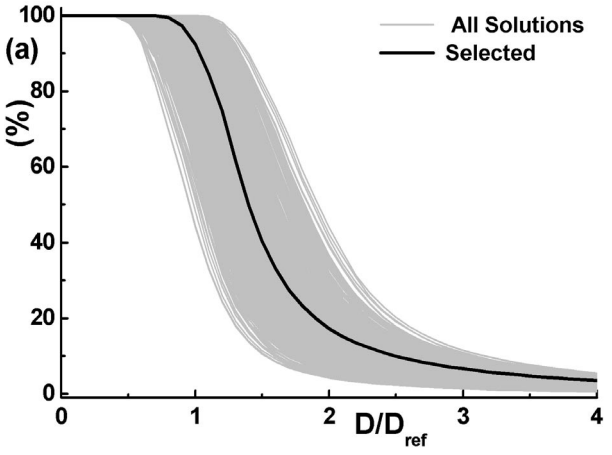

Figure 5a

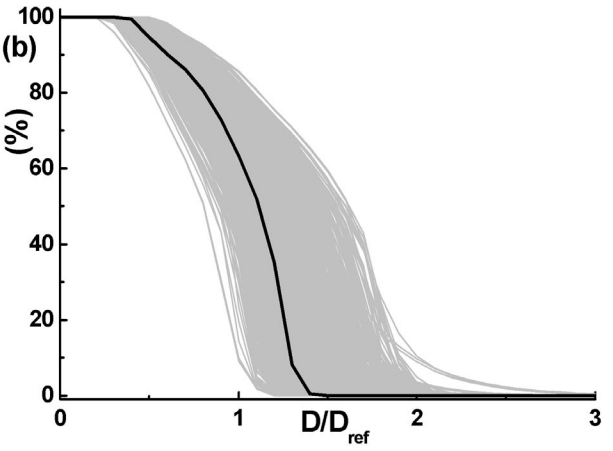

Figure 5b

Figure 5. Example of a plot of the DVHs (a) the PTV and for (b) the urethra obtained from a representative set of non-dominated solutions. A single solution selected by a treatment planner is shown. Its corresponding DVHs can be compared to the DVHS of the other solutions

The position of selected solutions can be seen in these projections. This helps to identify their position in the multidimensional Pareto front and to quantify the degree of correlation between the objectives and of the possibilities provided by the non-dominated set. The Pareto front provides information such as: How much can an objective be optimised and how this modifies the other objectives values? What is the range of values for each objective? The trade-off between other DVH derived quantities can also be used to select the optimal solution, see Figure 6.

Optimisation algorithms

There is no optimisation algorithm which is optimal for all optimisation problems.

The most important single and multiobjective optimisations algorithms used for optimisation of dose distributions in brachytherapy are.

– Deterministic. Optimisation methods that do not use any random elements during the optimisation. Linear programming and quadratic programming algorithms belong to this class.
– Stochastic. Optimisation algorithms that use random elements produced by the use of random numbers. Such algorithms are evolutionary algorithms and simulated annealing.

Linear and integer programming

In linear programming (LP) [17] certain variables should take integer values but for the sake of convenience, fractional values are taken assuming that the variables are likely to be so large that any fractional part could be neglected. While this is acceptable in some situations, in many cases it is not, and in such cases numerical solutions are required in which the variables take only integer values.

Problems in which this is the situation are called *integer program problems* and the subject of solving such programs is called *integer programming* (IP). IPs occur frequently because many decisions are essentially discrete (such as yes/no, 1/0) in that one (or more) options must be chosen from a finite set of alternatives.

For problems in which some variables can take only integer values and some variables can take fractional

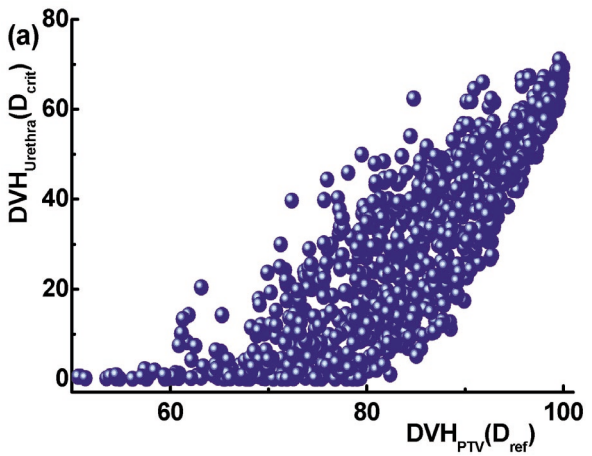

Figure 6a

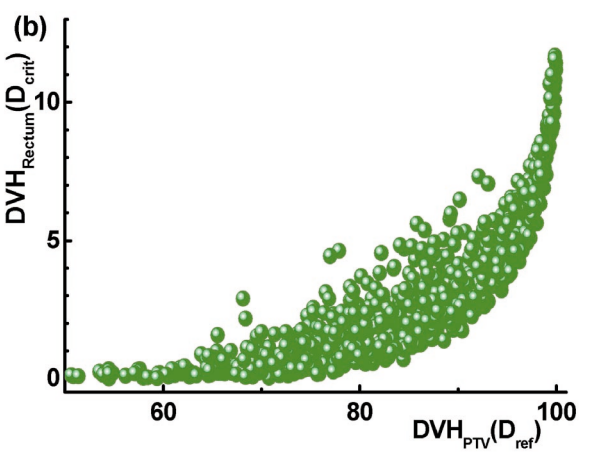

Figure 6b

Figure 6. Trade-off between DVH(D_{ref}) for the PTV and (a) volume of urethra with overdose, (b) volume of rectum with overdose

values are called *mixed integer problems* (MIP). The LDR dose optimisation problem can be considered as an *IP* problem where the parameters are 1 or 0 if a specified position has to be occupied by a source or not.

As linear optimisation methods do not necessary provide integer solutions a *branch and bound method* is used [18].

The method excludes from the search parts of the search space which cannot give better results than the current best known solution. Upper and lower bounds have to be specified for parameters for which no integer solution can be found. The problem is divided recursively forming a complex tree structure of sub-problems to be solved until a feasible solution is found.

Simulated annealing

For objectives that are not continuous and/or in the presence of local minima gradient-based algorithms can not be used or produce sub-optimal results.

In analogy with a technique known in metallurgy when a molten metal reaches a crystalline structure which is the global minimum thermodynamic energy of the system, if it is cooled slow enough, in simulated annealing (SA) an artificial temperature is introduced and gradually cooled. The parameter values (configurations) are produced randomly according to a so called *visiting probability distribution*. The cooling schema depends on the visiting probability distribution. In SA two consecutive configurations are compared. The temperature acting as a source of noise helps the system to escape from local minima. Near the end of the cooling process the system is hopefully inside the attractive basin of the global optimum. The challenge is to decrease the temperature fast enough without any irreversible trapping at any local minimum. The principal steps of a SA algorithm are shown in Figure 7.

Steps **3** and **4** of the algorithm, see Figure 7, allows to escape from local minima because not only configurations will be accepted that reduce the energy but also configurations that increase the energy (uphill moves). This depends on the temperature T(k). As the temperature is reduced only very small uphill moves are accepted. The search is more localized.

1. Get initial configuration S and temperature $T(0) = T_0$, set $k=0$
2. Select S' successor of S according to a visiting probability distribution
3. Calculate $\Delta E = E(S') - E(S)$
4. If $\Delta E \leq 0$ then set S = S' else set S=S' with probability $\exp(-\Delta E/T)$
5. If equilibrium at current T is reached then go to step **2** else go to step **6**
6. $k=k+1$
7. Reduce T according to the cooling schedule $T(k)$.
8. If stopping criterion satisfied go to step **2** else output best solution found

Figure 7. Principal steps of an SA algorithm

Evolutionary algorithms

Evolutionary algorithm (EA) is a collective term for all variants of probabilistic optimisation algorithms that are inspired by Darwinian evolution.

A genetic algorithm (GA) is a variant of EA, which, in analogy to the biological DNA alphabet, operates on strings which are usually bit strings of constant length. The string corresponds to the genotype of the individual. The phenotype of the individual is obtained by a mapping onto the object parameters (genotype-phenotype mapping). Usually a GA has the following components:
- A representation of potential solutions to the problem.
- A method to create an initial population of potential solutions.
- An evaluation function that plays the role of the environment, rating solutions in term of their fitness.
- Genetic operators that alter the composition of the population members of the next generation.
- Values of various parameters that the genetic algorithm uses (population size, probabilities of applying genetic operators, etc.).

In contrast to the canonical GA with bit encoded parameters, the genome of real-coded GA consists of real-valued object parameters, *i.e.* evolution operates on the natural representation. Usually for each chromosome an upper and lower limit of possible values is given which reduces the size of the search space.
- Fitness is an evaluation of an individual with respect to its reproduction capability and is usually a function of the objective function (to be optimised), which depends on the object parameters. The term *fitness function* is often used as a synonym for objective function.
- Selection in EA is based on the fitness. Generally, it is determined on the basis of the objective value(s) of the individual in comparison with all other individuals in the selection pool. In tournament selection a number T of individuals is chosen randomly from the population and the best individual from this group is selected as parent. This process is repeated as often as individuals to choose. These selected parents randomly produce uniform offspring. The parameter for tournament selection is the tournament size T. T takes values ranging from 2 to the number of individuals in the population. Increasing T increases the selection pressure, *i.e.* the probability of the best individual being selected compared to the average probability of selection of all individuals. Also the selection intensity increases, i.e. the expected average fitness value of the population after applying the selection method.
- Elitism is a method that guarantees that the best ever found solution would always survive the evolutionary process. For multiobjective optimisation elitism has to consider that a single optimum solution does not exist but a set of so-called non-dominated solutions.
- Crossover operators such as the simulated binary crossover (SBX) [19] allow the parameter space to be

searched initially sufficiently in large steps. During the evolution the search is limited around the current parameter values with increasing accuracy.
- Mutation operators have been proposed for real-coded GAs, such as the *Polynomial mutation* [20] and the *non-uniform mutation* [21]. Mutation searches usually in the local neighbourhood of the parent solution whereas crossover results in a more global oriented exploration of the search space.

An implementation of a GA begins with a population of (typical random) chromosomes. One then evaluates in such a way that those chromosomes which represent a better solution to a problem are given more chances to reproduce than those chromosomes which are poorer solutions. The goodness of a solution is typically defined with respect to the current population defined by a fitness function. Figure 8 shows the principal steps for GAs.

1. Initialise population chromosome values.
2. Assign fitness for each individual.
3. Select individuals for reproduction.
4. Perform crossover between random selected pairs with probability p_C.
5. Perform mutation with probability p_M.
6. Stop. If maximum generation reached or any other stopping criterion is satisfied else go to **2**.

Figure 8. Principal steps of a genetic algorithm.

Multiobjective evolutionary methods

Single objective optimisation algorithms provide in the ideal case only one Pareto optimal solution in one optimisation run. Multiobjective evolutionary algorithms (MOEAs) provide a representative set of the Pareto front. The following problems have to be considered
- How to maintain a diverse Pareto front approximation (Density estimation, Diversity).
- How to prevent non-dominated solutions from being lost? (Environmental selection).
- How to guide the population towards the Pareto front? (Mating selection).

MOEAs are mainly either aggregation or dominance based.
- Aggregation based – Non-dominated solutions are obtained by a weighted sum of the individual objective functions. The importance parameters can be varied during the evolution of the population and non-dominated solutions are acquired.
- Dominance based – MOEAs use in this case the dominance relation as a measure of the fitness of each individual. No parameters are required such as importance factors for aggregate-based algorithms.

A representative set of a finite number of solutions requires that the non-dominated solutions are as uniformly as possible distributed on the Pareto front of interest.

MOEAs can be more effective than multistart single objective optimisation algorithms. The search space is explored in a single optimisation run. It is easier to select a solution if alternatives are known. Aggregation of several objectives into a single one requires setting of parameters. True multiobjective evolutionary algorithms do not require importance factors.

LDR brachytherapy

The start of LDR inverse planning in the 1930s

Although a certain amount of work had been published earlier on the calculation of the distribution of exposure around a finite length linear source in air by Meyer & Schweidler (1916) [22] and Sievert (1921) [23], it was not until the 1930s that there were many publications on this topic which could lead to practical applications in the hospital. The majority were related to surface brachytherapy applicators, but volume implants were also considered to a certain extent.

Simple geometrical sources were considered: the line, annulus, disc, sphere and cylinder, all with uniform radioactive density per cm, per cm^2 or per cm^3, whichever was relevant to the geometry being considered. Several groups in the 1930s were attempting to develop a *System*, including those led by Murdoch in Brussels, by Mayneord at the Royal Cancer (later Marsden) Hospital in London, by Souttar at the London Hospital and by Paterson at the Christie Hospital & Holt Radium Institute in Manchester [24]. With hindsight we now know that Manchester *won* but it was not immediately apparent in the early 1930s that this would be the result.

The calculations started with the point source as a basic radioactive element of the geometry being considered. Then using the inverse square law and the k-factor for radium (in units of röntgen per hour per milligram at 1 cm) the exposure rate (X) at a distance r cm for a milligram radium point source was given by

$$X = k/r^2 \text{ röntgen / hour} \qquad (9)$$

One of the great debating points in the literature of 1930s was the numerical value of k, with the value of 9.0 R/hr/mgm used by Mayneord [25] and others from 1932, becoming 8.4 in the Manchester system [26] in 1967 for a point source filtered by 0.5 mm platinum. However, by the early 1960s it had been generally agreed that it was 8.25 and having had its name changed to specific gamma-ray constant (Γ) in the 1950s, it is currently called the exposure rate constant [27] (R/hr/mCi at 1 cm) although with SI units what is now more often quoted is the specific gamma-ray constant of $1.760X10^{-18}$ $Ckg^{-1}s^{-1}$ $Bq^{-1}m^2$ or the air kerma rate constant 0.195 μGy^{-1}

$MBq^{-1}m^2$. Mathematically the simplest linear source is infinitely thin and unfiltered, consisting of an infinite number of elementary linear sources (each consisting of a number of point sources). However, practical line sources always have a filter surrounding them to absorb the alpha and beta radiation and of course they are also of finite length.

If k is the k-factor, P is the point of interest in air at a distance from the linear source, r is the linear radioactive density, h is the perpendicular distance from the source to point P and X_p is the exposure at P the X_p is given by the equation

$$X_p = \frac{k\rho}{h}\left[Fn(\Theta_2) - Fn(\Theta_1)\right] \text{ röntgen / hour} \quad (10)$$

Where the functions $Fn(\Theta)$ which have been tabulated by Sievert [23, 28] over a wide range of parameters are known as the Sievert integrals, where

$$Fn(\Theta) = \int_0^{\Theta} \exp\left[-\mu \cdot d \cdot \sec(\Theta)\right] d\Theta \quad (11)$$

and μ is the linear attenuation coefficient of the platinum filter. The line source of finite length a is divided into an infinite number of elementary sources of length dx, where the filter is an infinitely long cylinder of radius d.

Figure 9 is a schematic diagram of a filtered line source and it can be seen that the surrounding space can be divided into four different regions A-D which are defined by the length of platinum filter traversed by the radium gamma-rays. For an end-on point, Q, in region C, where the maximum amount of platinum is traversed the exposure rate at Q is X_Q given by

$$X_Q = \left(\frac{k \cdot \rho}{h}\right) \int_{\Theta_1}^{\Theta_2} \exp\left\{-\mu \cdot \left[b - (a/2) - d - h \cdot \tan(\Theta)\right] / \sin(\Theta)\right\} d\Theta \quad (12)$$

where the integration limits are $\Theta_1 = \tan^{-1}\left[b - (a/2)\right]/h$ and $\Theta_2 = \tan^{-1}\left[b + (a/2)\right]/h$.

These Sievert integrals and the formulae given above are the first brachytherapy algorithms and were used for many years following the 1921 and 1932 publications of Sievert [23, 28]. Although some authors republished the Sievert integrals in a more convenient format for use than the original tables, devising for example, nomograms.

Sievert did not include any self-absorption correction to take into account the finite thickness of the radium source and also presented the integrals only for exposure in air and not for absorbed dose in water.

However, relatively shortly before the widespread use of digital computers for radiotherapy planning, Young and Batho published [30] in 1964 tables which took these factors into account. Using a factor of 0.97 to convert röntgens in air to rads in water they tabulated data for some 3000 points for each of several filtrations. However, with the availability of gamma-ray source dosimetry calculation software such extensive tables were no longer required and the modern era was entered.

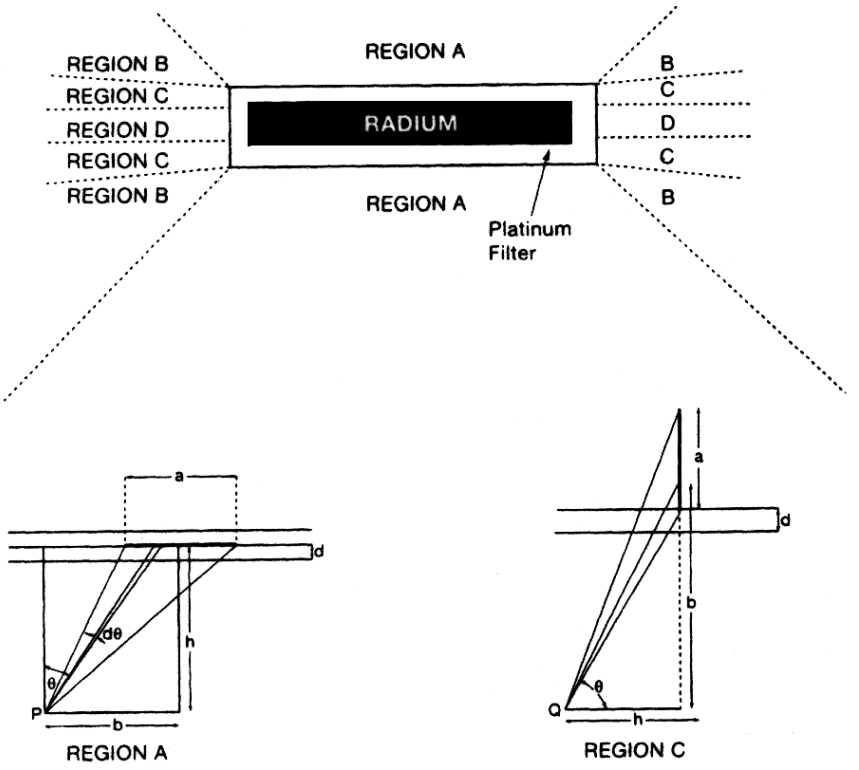

Figure 9. Regions of interest around a filtered linear radium source when it is required to calculate the exposure rate around the source [29]

The algorithms for calculating the exposure distributions in air around disc and annular sources were more complicated than those given above for a line source, but a judicious superposition of an annular source of uniform radioactive density ρ_A on a disc source of uniform radioactive density ρ_D a homogeneous exposure distribution could be found at a distance (say 1 cm) from the combination disc + annulus.

In this manner, a *System* could be devised for planar surface brachytherapy applicators and this is essentially what was proposed by Mayneord, Souttar, Paterson & Parker and others [29].

Spherical volumes are relevant to interstitial brachytherapy and the calculations for a *System* were approached in a similar manner to that described above, although in this instance, it was a combination spherical shell + sphere which was considered. The aim here was to obtain a homogeneous exposure throughout a sphere and the problem was to define the radius of the sphere and the thickness of the spherical shell.

One example is shown [29] in Figure 10 for a sphere of radius s cm and uniform radioactive density ρ_{Sphere}=1 Ci/cm^3 combined with a spherical shell of thickness 0.2a cm and radioactive density ρ_{Shell}= 3 Ci/cm^3. The exposure rates for the sphere alone are also shown in Figure 10.

The Manchester system prevailed in part because the energy of Ralston Paterson and in part because the Manchester physicists of the early 1930s undertook such detailed studies, publishing the first paper in 1934 for surface brachytherapy [31], in 1936 for cylindrical distributions [32], and in 1938 for both interstitial therapy [33] and intracavitary gynaecological applications [34].

Other attempts such as those of physicist Mayneord and the surgeon Souttar in London [29] were largely the work of one person and if only for this reason, could not compete with Manchester: although both published the basis of very practical systems.

In both the Manchester and Quimby systems the planning of an interstitial implant consists of determining the area or volume of a target region and then referring to a table or graph for the required total source strength (milligram-hours) per unit peripheral dose rate [35]. The

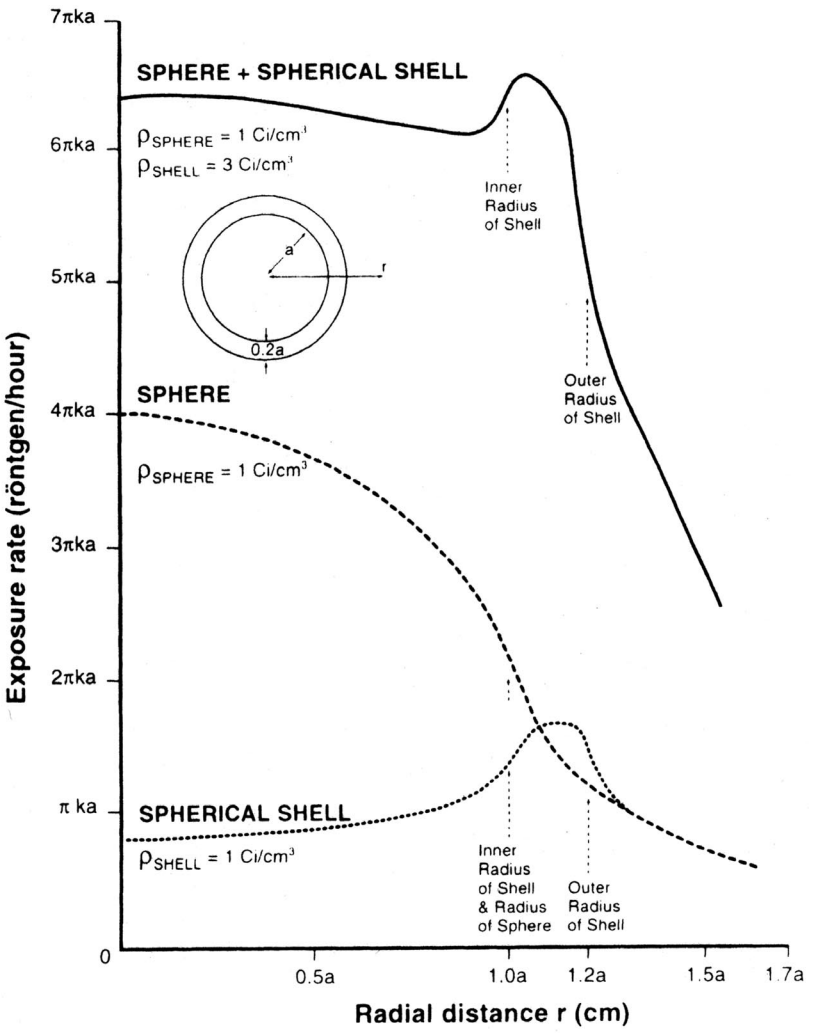

Figure 10. Exposure rate along the radii of a combined spherical source with different radioactive densities, showing an approximate homogeneous exposure rate for the sphere [29]. This represents a typical study in the period 1930-1935

objective of the interstitial system of Manchester is to deliver a homogeneous dose throughout the implanted region or in the treatment plane at 0.5 cm distance for planar implants.

The Quimby system (always more popular in the USA than in Europe) called for a uniform distribution of source strength and accepted the hot spots in the central region of the implant. The Quimby system prescribed dose was the same as the peripheral dose [35].

It is also noted that in brachytherapy inverse planning as well as in many other fields there are several instances of *reinventing the wheel* where earlier studies are ignored and later studies appear to be the first in their field. One such example is the work of Kneschaurek *et al* in 1987 [36] and Xio-Hong W and Potters in 2001 [37]. They reported that for a uniform distribution inside the sphere the activity density increases rapidly towards the surface of the sphere where it reaches infinity.

Davison (1950) [38] has solved the problem for a sphere and infinite cylinder and proved that the density ρ of radioactive material within the sphere must be a simple function of the radius, namely

$$\rho = \frac{1}{\sqrt{1-r^2}} \tag{13}$$

where r is the distance from the centre expressed as a fraction of the radius. Thus the density at the surface must be infinite to preserve the uniform field. This is the first exact analytical solution of this important problem that has been given [39].

To end this brief review it is interesting to relate the story of Jack Meredith [40], the editor of the standard Manchester system text [26] and Ralston Paterson's chief physicist following the departure to the USA of Herbert Parker. In the early 1930s Paterson had visited Brussels where work was being undertaken by Murdoch [41] on a radium *System*. Paterson was so impressed that he returned to Manchester with a few sketches, gave these to Parker and said "This will work, go away and prove it", which Parker duly did.

Current theoretical studies for LDR brachytherapy

Alfredo *et al* [42] used a back-projection algorithm and idealized ellipsoidal shapes for the PTV to obtain the activity distribution for an optimal dose distribution.

Theoretical work by Xio-Hong and Potters [37] is similar to the work of Kneschaurek *et al* [36], but they use a more realistic model for the radiation characteristics of the LDR sources. They examined the minimum quantity of radioactivity required to deliver a prescribed dose to a spherical PTV.

The dose rate delivered by a single source [37], is given by

$$\dot{D}(r) = \Lambda \overline{\phi}_{an} \frac{g(r)}{r^2} S_k \tag{14}$$

where Λ is the dose rate constant, $\overline{\phi}_{an}$ the anisotropy constant, S_k the air kerma strength and $g(r)$ the radial dose with the parameterisation $g(r)=c_1 \exp(-\mu_1 r)+c_2 \exp(-\mu_2 r)$. The parameters c_1, c_2, μ_1 and μ_2 are source-specific.

The integral dose delivered by a single source is

$$\varepsilon = 4\pi \cdot \Lambda \overline{\phi}_{an} S_k \left(\frac{c_1}{\mu_1} + \frac{c_2}{\mu_2} \right) \frac{T_{1/2}}{\ln 2} \tag{15}$$

where $T_{1/2}$ is the radionuclide half-life. Using a PTV approximated by a sphere of radius R, the *patient* integral dose E is $E=\pi/6R^3 D_{ref} F$, where D_{ref} is the prescribed uniform dose, F the ratio of patient integral dose to prostate integral dose. The patient integral dose is defined as the total energy absorbed in the patient body. This is the *so-called* therapeutic ratio.

"When the beam of radiation enters the patient, energy is absorbed not only in the tumour region but also in many other places. The total energy absorbed from the beam is *called* the *integral* dose and was originally defined by Mayneord in 1940 [43, 44]. It is desirable to keep the integral dose small while an adequate tumour dose is being delivered. An ideal situation, which can never be achieved, would be one in which all the absorbed energy was concentrated in the tumour and none absorbed elsewhere. This would give the minimum integral dose for a given tumour dose. The integral dose to a mass of tissue is the product of the mass of tissue and the dose which it receives. The unit of integral dose, defined by Johns & Cunningham in 1969 [45], is the gram·rad, where 1 gm·rad=100 ergs".

This definition is just as relevant for brachytherapy. Although the radioactive sources are generally inside the tumour region radiation will traverse also normal tissue and OARs. With the current units, the rad replaced by cGy and the unit of integral dose is 1 Joule.

For N implanted sources we have

$$\begin{aligned} E = N\varepsilon = E = \pi/6R^3 D_{ref} F = \\ = 4\pi \cdot \Lambda \overline{\phi}_{an} N S_k \left(\frac{c_1}{\mu_1} + \frac{c_2}{\mu_2} \right) \frac{T_{1/2}}{\ln 2} \end{aligned} \tag{16}$$

and the activity per unit dose is

$$N S_k / D_{ref} = \frac{R^3}{24 \cdot \Lambda \overline{\phi}_{an} \left(\frac{c_1}{\mu_1} + \frac{c_2}{\mu_2} \right) \frac{T_{1/2}}{\ln 2}} F \tag{17}$$

The question is which continuous source density $\rho(r)$ distribution produces the desired dose rate distribution. This can be solved by considering the integral equation:

$$\begin{aligned} \iiint dr \rho(r) \dot{K}(|\mathbf{x}-r|) = \dot{D}(x), \\ \dot{K}(|x-r|) = \Lambda \overline{\phi}_{an} \frac{g(|\mathbf{x}-r|)}{(|\mathbf{x}-r|)^2} \end{aligned} \tag{18}$$

The equation for a spherical prostate model results in an inhomogeneous Fredholm integral equation of the first kind. The solution of this equation can be described in a nomogram for source dimensions and a therapeutic ratio of the type $F = xR^y$, with F = 5.3 for ^{125}I (R=4 cm) and F = 2.7 for ^{103}Pd.

The resulting source density distribution provides an explanation for the choice of peripheral loading rule that is necessary to achieve an optimal dose distribution. Additionally a relationship between the total activity per unit dose (A) and radius of the sphere (R) is obtained using $A=cR^n$ where A is the total activity required per unit dose. The results quoted by Xio-Hong and Potters [37] are $A = 0.0098R^{2.09}$ U/Gy for ^{125}I and $A=0.031R^{2.25}$ U/Gy for ^{103}Pd. These parameters were compared to values recommended by AAPM TG 64 [46], namely (c, n) = (0.014, 2.05) for ^{125}I and (0.056, 2.22) for ^{103}Pd.

The possibility that the theoretical spherical model analysis leads to a smaller total activity required to deliver a prescribed dose when compared to AAPM recommended values is explained by the clusters of radioactive density in the seeds. Hence we have cold spots due to intersource spaces and hot spots around the sources, rather than a uniform spherical distribution of activity.

Strategy options for LDR brachytherapy

The strategy options in the 21st century for brachytherapy using seeds are as follows, using prostate cancer as an example. They follow directly from the earlier work starting in the 1930s and are also analytical methods.

- Distribute in the peripheral zone particularly to reduce the dose around the urethra. Minimum peripheral dose is used to specify treatment dose.
- Distribute seeds uniformly to minimize cold spots. This approach could produce high dose values in the centre of the implant.
- Avoid some of the seeds in the centre of the implant in order to reduce high dose values. This defines a modified peripheral loading method.

Some studies, such as that of Butler *et al* [47] take the PTV dose distribution as a starting point and compare the dosimetric results from different loading strategies. They considered three different peripheral loadings arrangements and found one of these to be stable to a certain extent to seed displacement. Basically this was only a trial and error study.

Computer-based inverse planning for LDR brachytherapy

Starting from the 1930s, inverse planning used geometrically derived rules to determine how to place the sources in order to achieve a uniform dose distribution of a specific level in planes, spheres and cylinders. These rules were obtained by calculating analytically the dose distribution and by using different source distribution parameters which were varied until an optimal distribution was obtained.

With the current 3D imaging technologies such loading/placement strategies are now, in many centres, altered to accommodate the real 3D anatomy of the PTV and of the OARs. However, the greatest activity density is virtually always around the periphery, see Eq. 13, [38].

With the wide availability of personal computers and the rapidly increasing computer power we have now entered the new era of *computer-based inverse planning* in brachytherapy. This inverse planning is now an optimisation process adapted to the individual geometry of the patient. Computer-based inverse planning does not require analytical models for the determination of a optimal number of sources, catheters and their position. It also considers various effects such as stability of solutions for seed misplacements which cannot ever be solved analytically without gross simplifications.

Initially the optimisation methods used simulated annealing (SA) and idealised PTV geometries and ignored OARs. However, new inverse planning optimisation algorithms are anatomy-based. Also, in the last few years multiobjective inverse planning algorithms have been developed which recognise the multiobjective optimisation problem which is inherent in inverse planning in brachytherapy [11, 12].

Iterative geometric optimisation

Y. Chen *et al* [48] generate optimised seed distributions by an iterative algorithm that is used to place one seed at a single step. The dose distribution in the PTV is calculated at each step to determine the coldest spot which is where the next source will to be placed. In this manner the dose uniformity throughout the PTV is continually improved as the source placement proceeds.

At each step, the total activity required for the seed configuration is calculated by normalizing the minimum dose to the prescribed dose. An optimised configuration is the one that takes the minimized total activity. That is, until SMPD has been minimized: where SMPD is the total source strength required to achieve 1 Gy in the minimum peripheral dose (MPD).

The minimum total activity required varies only very slowly with the number of seeds. Hence multiple clinically acceptable seed configurations with a similar total activity but with different individual activities are generated using this geometrical optimisation strategy as shown in Figure 11. The computer generated treatment plans produce solutions where most of the seeds are distributed in the periphery of the target. This is a similar result to that determined by Paterson and Parker in their Manchester system for rules for a volume implant.

The first seed is placed randomly at an allowed source location within the specific template geometry. The doses given by this source with unit strength to all the points in calculation grid are then calculated. The source activity is then scaled by matching the minimal dose within the target volume to the prescribed dose. This

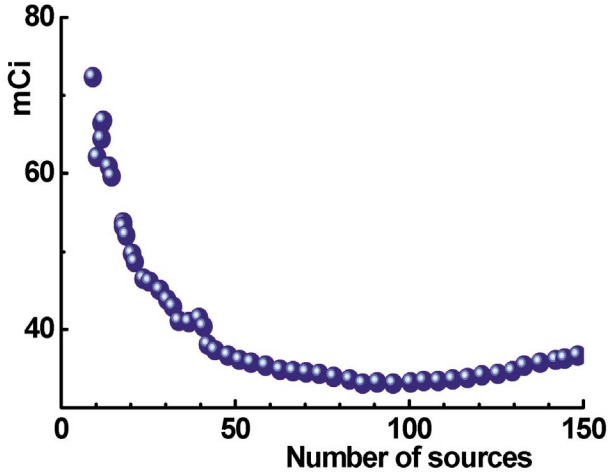

Figure 11. Total source activity required to deliver a specific dose to the MPD as a function of the number of the seeds implanted, after *Chen et al* [48]

1. Set allowed needle positions
2. Initial number of seeds based on prostate volume. Set $k = 0$ and $T = T(0)$. Generation of an initial seed configuration $S(0)$.
3. Get initial configuration S and temperature $T(0)=T_0$, set $k=0$
4. Select S' successor of S by replacing 1-2 seeds.
5. Calculate $\Delta E = E(S') - E(S)$
6. If $\Delta E \leq 0$ then set S = S' else set S = S' with probability $\exp(-\Delta E/T)$
7. If equilibrium at current T is reached then go to step **4** else go to step **8**
8. $k=k+1$
9. Reduce T according to the cooling schedule $T(k) = T(0)/k$.
10. If stopping criterion satisfied go to step **4** else output best solution found

Figure 12. SA algorithm for LDR inverse planning [51]

would be the total activity required if only one seed were to be implanted.

Next, a second source is placed at a seed location closest to the coldest spot inside the PTV caused by the first source. The dose at all calculation points is then computed for the first two sources, each with unit activity. This iterative procedure is repeated until some 100 seeds are positioned within the dimensions of the template. The total activity is determined by normalizing the minimum dose to the prescribed dose.

The seed configuration for an actual implantation is chosen from the sequence generated by iteration such that the total activity is close to the minimized value and an available individual activity is matched.

Inverse planning with simulated annealing

Ron Sloboda was the first author to use an SA algorithm for LDR brachytherapy inverse planning [49, 50]. The square root of a quadratic objective function was used, including lower and upper dose penalty terms. Integer parameters were also used and the visiting probability distribution considers moves such as an increase or decrease of numbers and/or positions of sources at a specified set of possible positions. By including weights at the source positions the method could also be used for HDR brachytherapy inverse planning.

Pouliot *et al* [51] also proposed a SA algorithm for LDR prostate brachytherapy inverse planning. The algorithm is described in Figure 12.

The optimisation requires 20,000 iterations. Empirically determined importance factors are used for the individual objectives. If the result is not satisfactory then a new set of importance factors is used and the optimisation is repeated again. Each optimisation run requires less than 1 minute.

Inverse planning with evolutionary algorithms

Yang *et al* [52] used variants of an elite single objective genetic algorithm with quadratic dosimetric objective functions. A small population of 25 members was used for the GA and single point crossover was performed. The PTV was approximated by an ellipsoid. Comparisons of the optimisation results of the GAs were made with manually optimised implants using as criteria the conformation number CN and the dose non-uniformity ratio DNR. If the dose in the urethra was not acceptable the optimisation was repeated with modifications to the importance factors until a satisfactory result was achieved. For a given set of catheters the number of sources and their optimal position were determined.

Yu and Schell [53] used a single objective genetic algorithm for idealized elliptical PTV geometries with half-axes a, b, c and an average dimensional index d=(a+b+c)/3. The fitness f(i) of the ith individual combines the number of needles N_n, the PUN and $S_{10\,mPD}$, *i.e.* the total source strength to deliver 10 Gy to the MPD point.

$$f(i) = \frac{\exp\left[A\left(\langle S_{10\,MPD}\rangle / S_{10\,MPD}(i)\right)\right](PUN)^{B}}{\left[\max\left(N_n, D\cdot d\right)\right]^{K}} \qquad (19)$$

A, B, D, K are parameters to control the individual objectives and $\langle S_{10\,mPD}\rangle$ is the average value of $S_{10\,mPD}$ over the population.

Decision steered algorithm

Yu *et al* [54] presented an a priori multiobjective GA for LDR prostate brachytherapy inverse planning. For the optimisation a total of 11 objectives f_1–f_{11} were defined.

- f_1 is the total source strength (U) required achieving 1 Gy of the MPD.
- f_2= 1/PUN.
- f_3–f_5 are the maximum critical dose values to the OARs (urethra, rectum bladder) normalized to the MPD.

– f_6–f_{10} are the expectation values of f_3–f_5 after random displacement of seeds from the intended positions.
– f_{11} is the number of used needles.

A genetic algorithm is used which is guided by artificial intelligence according to requirements of the treatment planner [16, 54]. The algorithm modifies the ranking when goals are achieved by reducing the search space and increases the search in a specific direction if the satisfying conditions are not met. A two-dimensional encoding of the catheter positions is used. The crossover point is individually selected for each catheter row on the template. This permits a more flexible exchange than when using a linear chromosome, see Figure 13.

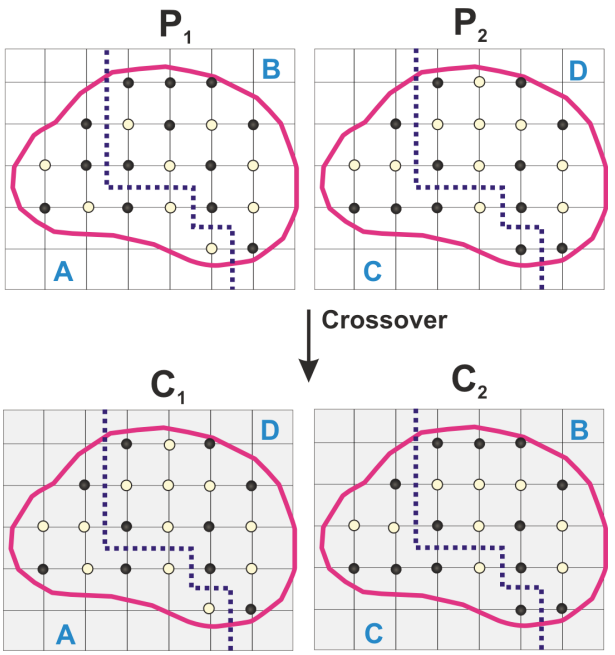

Figure 13. Crossover of the two-dimensional chromosome for template based LDR inverse planning using the method proposed by Yu *et al* [54]. The individual parent solutions P_1 and P_2 after crossover produce the children solutions C_1 and C_2. The contours of the PTV are projected onto the template plane

Ranking among a group of candidate plans is based on a weighted L_p distance metric. The ideal vector $f^+=\left(f_1^+,f_2^+,...,f_{11}^+\right)$ and anti-deal vector $f^-=\left(f_1^-,f_2^-,...,f_{11}^-\right)$ are calculated.

The distance of the ith individual to the ideal and anti-ideal point using the L_p weighted metric $L_p^+(i)$ is $L_p^-(i)$ and respectively.

$$L_p^+(i)=\left(\sum_{j=1}^{M} g_j(t)\left(f_j(i)-f_j^+\right)^p\right)^{\frac{1}{p}} \qquad (20)$$

$$L_p^-(i)=\left(\sum_{j=1}^{M} g_j(t)\left(f_j(i)-f_j^-\right)^p\right)^{\frac{1}{p}} \qquad (21)$$

$g_j(t)$ is the metric weight for the jth objective at generation t. Various values for p, p=1,2,...,∞ have been tested. The metric is used to rank individuals a higher rank defines a more preferred plan. The rank of the ith individual $R_p(i)$ is

$$R_p(i)=\frac{L_p^-(i)}{\left(L_p^+(i)+L_p^-(i)\right)} \qquad (22)$$

The user is required to present before optimisation the set of importance factors for the jth objectives W_j and goals or satisfying conditions G, S for the objectives. If a goal G_k for the kth objective is satisfied and further optimisation makes the decision indifferent to the outcome then f_j^+ is replaced by G_k in the metric L_p^+. A satisfying condition S_k is specified if a minimum preferred level of achievement exists for the k^{th} objective. If the current best outcome f_k^+ is less preferred to S_k then $g_k(t)$ is increased temporarily by a factor $B(t)=1+B_0\exp\left(-\varepsilon(t)\right)$.

The function $\varepsilon(t)$ is taken by Yu *et al* [16] to be "realizations of the state energy of the decision system following a Boltzmann distribution at temperature $T(t)$, which undergoes thermodynamic cooling, $T(t)=T_0/(1+t)$". This is analogous to simulated annealing.

The metric weights are $g_j(t)=W_j+u_j(t)$ where $u_j(t)$ is a normal distributed random variable with mean=0 and variance $W_j\left(1-\exp\left(-\varepsilon(t)\right)\right)^2$. This approach considers the judgment and preferences of a treatment planner. Objectives f_6–f_{10} are included to solutions that are more robust to seed misplacements.

The algorithm is shown in Figure 14. A population of 64 individuals is selected and random activity loadings for the catheters are selected, including preferentially peripheral patterns.

A stopping criterion considers if after some specified number of iterations no improvement is observed. The selection method uses a dynamic tournament scenario in which the number of parents used for the selection increases periodically during the optimisation, therefore increasing the selection pressure.

1. Initialise population with random loading patterns.
2. Evaluate dosimetry for each individual.
3. Rank individuals according to a multiobjective metric (see Figure 15).
4. Perform a dynamic n-Tournament. The n best individuals are selected for reproduction. This number increases periodically by one unit reaching finally 25% of the population size.
5. Perform crossover.
6. Perform a flip mutation. If a catheter is selected for mutation its on/off status is flipped.
7. If generation maximum reached or other criterion is satisfied output solution else go to **2**.

Figure 14. GA inverse planning algorithm for LDR, after Yu *et al*. [54]

The ranking of the individuals is described in Figure 15.

1. Evaluate N individuals of M-tuples of objectives $f_j(i)$, $i=1,...,N$ and $j=1,...,M$
2. For all M objectives calculate f_j^+ and f_j^-.
3. For all M objectives set $g_j(t)$
4. For all $j=1,...,M$ objectives if S_j is defined and preferred to f_j^+ set $g_j(t)=B(t)g_j(t)$
5. For all $j=1,...,M$ objectives if G_j is defined set $f_j^+=G_j$.
6. Compute $L_p^+(i), L_p^-(i), i=1,...,N$
7. Compute $R_p(i), i=1,...,N$

Figure 15. Ranking of the individuals

Inverse planning with mixed integer programming

A linear mixed integer programming MIP algorithm was proposed by Lee *et al* [55] for LDR prostate brachytherapy inverse planning. A system of linear constraints is imposed which attempts to keep the dose level at each sampling point to within specified bounds. A grid of possible seed placement positions is considered and the parameters 0/1 at these specify a placement or not of a seed. These are the integer parameters of the problem.

Constraints of dose values define the real continuous parameters of the problem. Each constraint uses a variable that either records if the desired constraint is satisfied, or the degree of the constraint violation. These additional variables are embedded into an objective function to be optimised. Two methods were used for the optimisation: (i) a branch and bound algorithm and (ii) a genetic algorithm.

Results of both methods for a data set of 20 prostate tumour cases indicate that both optimisation algorithms are capable of producing good solutions in 5-15 min. It was also found that small variations in model parameters can have a measurable effect on the dose distribution of the resulting plans [55].

In this study the authors let $d(P)=\sum_{j=1}^{M}\tilde{d}_{Pj}x_j$ be the dose at point P. $\tilde{d}_{Pj}$ is the dose contribution of the jth seed position to the point P, x_j 0/1 variables indicating the presence of a seed at the jth possible seed position. Let L_p and U_p be the upper and lower dose value bounds desired at the point P. The following constraints are considered.

$$d(P)+N_p(1-v_P)\geq L_p \quad (23)$$

$$d(P)+M_p(1-w_P)\leq U_p \quad (24)$$

Positive constant terms M_p, N_p are included for the lower and upper bound, v_P and w_P are 0/1 variables. If $v_P=1$ can be found then the lower bound constraint is satisfied and for $w_P=1$ also the upper bound. The objective is to maximize the number of points which satisfy the lower and upper constraints *i.e.* maximize $\sum_P(v_P+w_P)$.

As it may difficult to satisfy constraints for some points a weighted sum can be used, and the objective is to maximize

$$\sum_P(a_Pv_P+\beta_Pw_P) \quad (25)$$

where(a_P,β_P) are non-negative real parameters.

In the second approach Lee *et al* [55] considered the deviation of the dose level at each point P from its bounds y_p, z_p are continuous parameters that are used the describe the violation of the constraints

$$d(P)+y_p\geq L_p \quad (26)$$

$$d(P)-z_p\leq U_p \quad (27)$$

The objective is to minimize the weighted sum of deviations

$$\sum_P(a_Py_P+\beta_Pz_P) \quad (28)$$

where (a_P,β_P) are non-negative real parameters.

Souza *et al* [56] also proposed an MIP algorithm and the branch and bound method for LDR prostate brachytherapy inverse planning. Dose optimisation constraints were imposed on a very fine dose grid (1 mm) within the target and OARs. In three-dimensions the number of continuous variables (dose calculation points) within the prostate alone exceeded 10,000, while the total number of dose points in the ultrasound image exceeds 100,000.

The fine sampling of the space in which dose is calculated leads to a large and complex mathematical model that is difficult to be solved as a three-dimensional problem. Even with state of the art branch and bound software it is not possible to solve the corresponding 3D mixed integer model. An iterative sequential optimisation method was developed, in which the seed placements within 2D ultrasound slices (planes) is optimised, taking into account dose contributions from neighbouring planes.

Within each 2D ultrasound image plane there are 156 potential implantation sites. However, since seeds can only be placed within the PTV, this number is reduced to 30-60 seed implantation sites per plane. Therefore the 0/1 (where 0 indicates there is no seed implanted and 1 indicates that there is a seed implanted) seed placement parameter must be determined for approximately 450-800 places in the template. This corresponds to the possible implantation sites over the entire PTV. There are typically 10-15 planes. With this method it is possible to obtain solutions in 20-45 min using a 200 MHz processor.

A comparison with a manual trial and error approach shows that the optimised plans are generally superior. If the dose to the urethra is undesirably high, a refined optimisation approach is used that lowers urethra dose without significant loss in target coverage.

The latter approach requires 5-10 min of additional computing time, much less than the manual approach with an average planning time of 2.5 hours.

Souza *et al* [56] implies that an analysis of the sensitivity of the optimised plans to seed misplacement during the implantation process indicates a remarkable stability of the dose distribution in comparison to manual treatment plans.

HDR brachytherapy

In HDR brachytherapy the optimal position of catheters and their position have to be found. For this process, the optimisation has to consider combinations of 5-20 catheters from a set of up to 60 possible catheters. For each catheter more than 20 source-dwell positions could exist. Additionally to the catheters the optimum dwell times at the dwell positions of each selected catheter have to be found.

The combinatorial complexity of this problem is extremely high. In LDR brachytherapy the seed sources are usually of the same activity. However, in HDR brachytherapy the variable dwell time produce a large number of solutions with different numbers and positions of catheters but with similar dose distributions. It should also be emphasised that the variation of the LDR seed positions in permanent brachytherapy and other effects such as post-implant oedema can greatly influence the final dose distribution and reduce the quality of the LDR results obtained by inverse planning.

Changes of source positions after implantation in HDR brachytherapy from the positions used in inverse planning are less important as modifications of the dwell times from post-planning optimisation can to some extent compensate for these factors.

We limit our discussion to the case where the possible catheter positions are defined by a template, usually by coordinates on a rectangular grid. We ignore the problem of the case where the catheters are not parallel to each other and have been positioned by *free-hand* implantation.

Empirical loading methods

The use of empirical derived methods is very common for the selection of catheters. Similar to the LDR brachytherapy situation, these HDR methods use a majority of peripherally placed catheters in order to achieve a uniform dose distribution. Sometimes the term *modified peripheral* is employed to infer that the PTV is large enough to justify a few centrally placed catheters.

The William Beaumont template-based method (WBT), [57] for inverse HDR prostate planning is one such an empirical method, derived from the analysis of a large number of clinical implants.

The catheter placements consider the reference plane lying between the base plane and apex and it is normally the plane with the largest prostate cross-sectional contour. The WBT method considers the geometrical dose optimisation method to be a basis for dose optimisation: the results strongly depend on the catheter geometry. The original WBT method assumes a cylindrical prostate geometry.

The prostate is defined on the reference plane and this contour is extrapolated and expanded between the base plane and the apex. Some parameters that must be specified are the distances between the peripheral catheters, and the urethra avoidance distance that catheters should have from the urethra.

The area and prostate perimeter at the reference plane defines the number and the position of internal catheters that will be placed additionally to the peripheral catheters. Depending on the prostate area 0, 2, 4 or 5 interior/central catheters are inserted additionally to the peripheral catheters. Their position is determined depending on their number, using the centre of the area and the bounding rectangle of the prostate contour.

Computer based methods

Multiobjective evolutionary inverse planning

For HDR brachytherapy inverse planning it is more natural to use multiobjective evolutionary algorithms (MOEAs) to obtain a representative set of non-dominated solutions rather than only a single solution.

The following set of objectives was used:

- $f_L^{PTV} = \frac{1}{N_{PTV}} \sum_{i=1}^{N_{PTV}} \Theta\left(D_L^V - d_i\right)$ as the fraction of PTV with a dose value $D < D_L^V$
- $f_H^{PTV} = \frac{1}{N_{PTV}} \sum_{i=1}^{N_{PTV}} \Theta\left(d_i - D_H^V\right)$ as the fraction of PTV with $D > D_H^V$
- $f_{OAR}^j = \frac{1}{N_{OAR}^j} \sum_{i=1}^{N_{OAR}^j} \Theta\left(d_i - D_{crit}^j\right)$ as the fraction for the jth OAR with $D > D_{crit}^j$
- $f_{NT} = \frac{1}{N_{NT}} \sum_{i=1}^{N_{NT}} d_i^2$ as the average squared dose in the surrounding normal tissue
- $f_N = N_C$ as the number of catheters N_C.

$D_L^V = D_{ref}$ is the prescription dose, or lower dose limit and D_H^V is the high dose limit in the PTV. f_{NT} is the mean quadratic dose in the surrounding normal tissue. N_{PTV}, N_{NT} and N_{OAR}^j are the number of sampling points in the PTV, normal tissue and in the jth OAR. The objectives, f_L^{PTV}, f_H^{PTV} and f_{OAR}^j are proportional to the DVH values at the corresponding dose values.

The advantage of using these objectives is that the results in terms of objective values are more intuitive to understand than other objectives. The use of the square of the dose value ensures that high dose values are more

likely to be avoided in the NT than are the more uniformly distributed moderate dose values. For D_H^V we use a value of 1.5 times the prescription dose. The dose is not normalized on any particular point or set of points.

In addition to the dosimetric objectives, the additional objective of the number of catheters is also included.

An automatic template-based catheter placement algorithm has been developed by Baltas and Lahanas for inverse planning in HDR brachytherapy. The algorithm determines from the anatomical structures, PTV and OARs which catheters and to what depth in the PTV they should be inserted, given a minimum distance to the PTV surface and OARs.

The part of each catheter that is inside the PTV can be adjusted individually according to the anatomy. The part of catheter that remains free in front of the template is called the *free length* and has to be at least as large as the afterloading system-dependent minimum free length. This is to ensure that the catheter can be connected to the transfer tube.

The adjustment of the catheter position (depth) at a specific template hole is performed by checking the minimum distance between the first dwell position of the catheter and the organ surfaces (PTV and selected OARs). That distance should be larger than a specified lower limit. The first SDP (the one that is closer to the catheter tip) must always be a feasible SDP. This means it must fulfil the above constraint. However, if the maximum number of potential active SDPs on a catheter is smaller than a specified minimum, the catheter will be rejected.

Hybrid evolutionary multiobjective optimisation

For the inverse planning we use a modified version of an algorithm proposed by Lahanas *et al* [12] for dose optimisation.

The MOEA is supported by a deterministic gradient-based optimisation algorithm and provides a representative set of non-dominated solutions. This set contains information for the treatment planner, such as how the results depend on the number of the catheters, the spectrum of DVHs for the PTV and the OARs. Additionally the corresponding trade-off between the objectives and the limitations of the dose distributions can be extracted. This data is used for the selection of a solution with a optimal number of catheters, their position and the smallest compromise on the individual objectives.

The initial random generated *NSGA-II* population moves fast towards the global Pareto front but slows down providing only a local Pareto front, see Figure 16. The global Pareto front can be reached if at all only asymptotically after a very large number of generations.

If a small number of individuals are moved on the global Pareto front, see Figure 16, using an efficient optimisation algorithm, then they efficiently attract the other individuals in their neighbourhood. These so-called *supporting solutions* [58, 59] improve very significantly the performance of MOEAs and enable a fast accumulation of solutions close to the global Pareto front. A combination of *NSGA-II* with a deterministic algorithm improves the diversity along the front and guides the population closer and faster towards the global Pareto front.

If the Pareto front is very large then for a small population, some important parts of the Pareto surface may not be occupied. It is possible to use constraints which allow restricting the population into parts of the objective space which are of particular interest. Such a constraint when used for the DVH-based objectives is $f_L^{PTV} < 0.3$, *i.e.* only solutions with a PTV coverage of at least 70% are considered. An archiving method in which an external population is filled with all the non-dominated solutions found can be used to accumulate a sufficient large number of solutions.

At each generation, each solution of the genetic population is compared with all the individuals of the external population. If a solution for the genetic pool dominates solutions for the external population and if it is non-dominated by them then it is added to the external pool and all the dominated solutions are removed. If the population has reached its maximum size, as set by the user, then the non-dominated solution replaces a solution that has the highest number of individuals in its neighbourhood.

This mechanism prevents accumulation of solutions in a part of the objective space and allows a more uniform coverage of the Pareto front by the archived solutions. The non-domination tests usually require much less time than the function evaluation and the non-dominated sorting. More than thousand non-dominated solutions can be acquired in 100 generations in one minute.

Encoding

For the inverse planning problem encoding a two-component chromosome is used. The first part W contains the dwell times of all dwell positions with a double precision floating-point representation. The second part C is a binary string which represents the catheters which have been selected: the so-called active catheters. The SDPs of the *active catheters* are called *active SDPs*.

Figure 16 shows the encoding for a five-catheter case. The dwell times of each catheter is saved in the arrays $\mathbf{w}_1,...,\mathbf{w}_5$. The catheter part encodes the case where catheters 2, 4 and 5 have been selected.

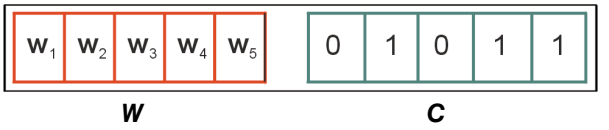

Figure 16. Encoding of the chromosomes for an *imaginary* treatment case with five possible catheters out of which three are used

Genetic operators

For the chromosome part *W* two crossover operators are used. For *W* a SBX crossover operator is used. For the second part *C* a two-point crossover operator and a flip mutation is used. A repair mechanism keeps the number of selected catheters inside a user specific range.

Tests with implants using the same importance factors but with a different number of SDPs show that the sum of the dwell times of all sources is almost constant. In the crossover of dwell times between solutions with a different number of active source-dwell positions we have to consider that the average dwell time is inversely proportional to the number of SDPs in the active catheters.

The exchanged information from crossover between individuals with different numbers of active SDPs has to be made independent of the number of active SDPs. Therefore the weights of each population member are multiplied by the number of active dwells decoded in the catheter chromosome. After the crossover the mutation is applied. This may change not only the catheter topology but also the number of catheters.

The weights after the genetic operations are divided by the actual number of active SDPS encoded in the catheter chromosome so that the dwell times depend on the number of active SDPs. Without this modification before the crossover and after the mutation, only solutions with the smallest possible number of allowed SDPs would be accumulated. Individuals with a larger number of active SDPs would contain after crossover the dwell times obtained by solutions with a smaller number of sources which are too high for these solutions. The resulting variances would so large that these individuals would not be selected.

A multiobjective evolutionary optimisation algorithm is used, see Figure 17. The user specifies a range of number of catheters to be considered. The optimisation algorithm requires 1-2 minutes on a 1.4 GHz PC to obtain a representative set of up to 100 solutions. Constraints are applied on the resulting solutions to avoid clinical not acceptable solutions.

1. Determine set of all allowed catheters.
2. Initialise individuals with solutions from a global optimisation algorithm.
3. Selection based on constrained domination ranking.
4. Perform a SBX crossover for the SDP weights chromosome and one point crossover for the catheter chromosome with rescaled dwell times.
5. Perform a polynomial mutation for the SDP weights chromosome and flip mutation for the catheter chromosome with rescaled dwell times.
6. Perform a repair mechanism to set the number of used catheters of each solution in a given range.
7. Reset scaling according to number of active SDPs.
8. Evaluate dosimetry for each individual.
9. If generation maximum or other criterion is satisfied output set of non-dominated solutions else go to **3**.

Figure 17. MOEA inverse planning for HDR brachytherapy

The analysis of these solutions, calculation of DVHs, and other dosimetric quantities such as COIN distributions and natural dose-volume histograms requires additional one minute. Decision making tools are used to analyse the trade-off between the objectives, compare DVHs of the PTV and the OARs and analyse range of dosimetric values. This information is used by a treatment planner to select the solution with the smallest compromise on the various objectives and which satisfies as best as possible clinical defined constraints.

Is inverse planning for HDR brachytherapy really necessary?

For HDR brachytherapy the optimisation of dwell times allows the optimisation of dose distribution even if the catheter and SDP geometry are not exactly as used in the inverse planning. Is inverse planning for HDR brachytherapy therefore really necessary?

Dose optimisation was performed by a treatment planner using the Nucletron PLATO treatment planning system. Three HDR plans were created with respectively 4, 10 and 16 catheters. The position of the catheters was determined by a trial and error method.

The HDR results were compared with those for a LDR plan using 29 catheters. They show that a large number of catheters are not necessarily a guarantee of a good optimisation, see Figure 18. Increasing the number of catheters and SDPs produces by geometric optimisation a number of hot spots. From dose point optimisation algorithms, by increasing the number of catheters, the number of negative dwells is increased and this reduces the quality of the solutions. The catheter position is important if good solutions with a small number of catheters have to be found. The dwell times cannot compensate for non-optimal catheter placements.

Tests show that the number of catheters can be reduced significantly without any important modification of the dose distribution. Inverse planning offers the possibility to reduce the number of catheters and simplify the treatment plan. MOEA inverse planning also offers important information for the selection of the best solution.

What can we learn from multiobjective inverse planning?

Multiobjective inverse planning offers a spectrum of possibilities and allows better understanding of the limitations and differences of optimisation methods. In the past, comparisons of different optimisation methods were made which were based on single solutions selected with some set of importance factors.

In LDR brachytherapy studies considered the differing results using ^{125}I and ^{103}Pd seeds. Despite their energy and half-life differences no conclusions have been made in terms of clinical benefits for ^{125}I versus ^{103}Pd.

Cha *et al* [60] did not observe any difference in clinical effectiveness but mentioned that there is

215

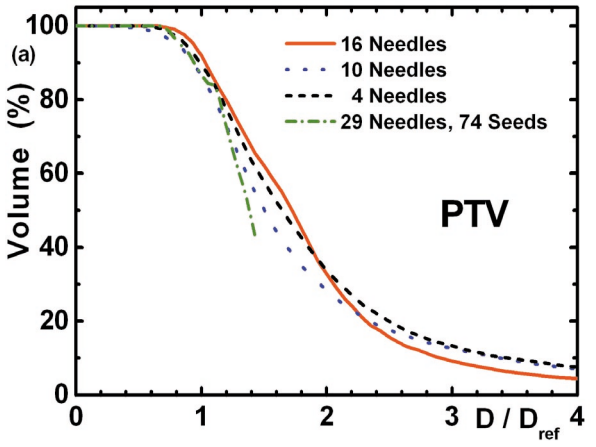

Figure 18.a

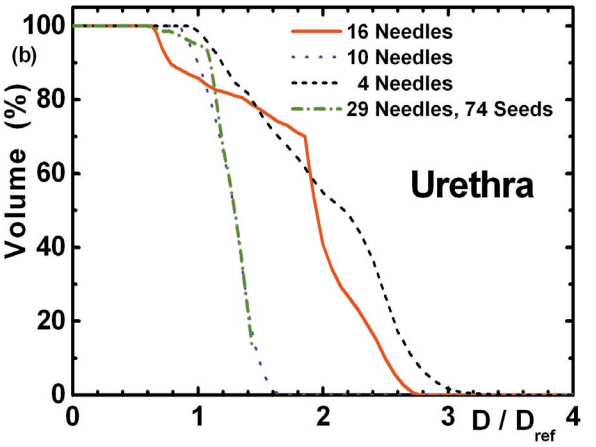

Figure 18.b

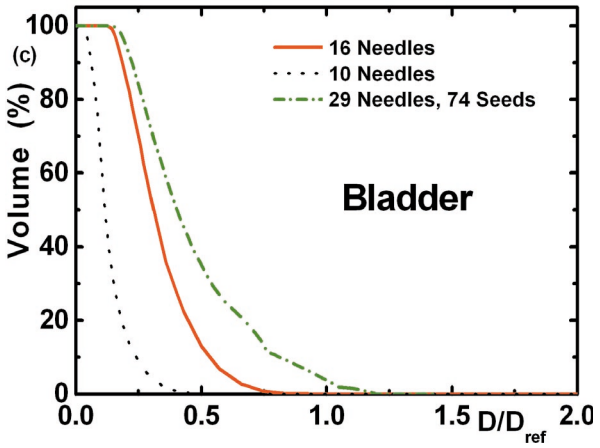

Figure 18.c

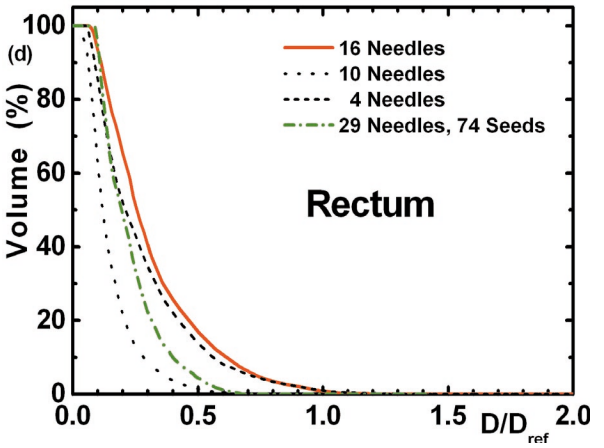

Figure 18.d

Figure 18. DVHs for (a) the PTV, (b) urethra, (c) bladder and (d) rectum for a prostate tumour patient. The results of an HDR dose optimisation using 4, 10 and 16 catheters are shown. The HDR results are compared with those for LDR brachytherapy with 29 catheters and 74 seeds

a considerable variability in the delineation of tumour volume and implant quality depending on the treatment planner. This makes conclusions difficult.

As the trade-off between the objectives is not known by the single objective optimisation algorithms used in the past we cannot say how good is a given solution as we do not know what part of the Pareto front it represents. Multiobjective optimisation offers this knowledge and as an example we examine how and if the solutions depend on the characteristics of a source for HDR brachytherapy.

Optimal sources for optimal results

The dose distribution depends on the characteristics of the sources, such as type of emitted radiation, its energy spectrum and the geometry of the source, including the material such as the encapsulation of the source. Even if there is a dominant inverse square dependence on the dose in brachytherapy, the possible dose distributions which can be obtained depend on the physical characteristics of the sources. The radial dose function g(r) for various monoenergetic point sources is shown in Figure 19(a). The radial distribution for a point source for various isotopes taking the mean energy is shown in Figure 19(b).

We consider monoenergetic point sources and the dependence of the optimisation results on the energy of the sources. For a prostate implant with 15 catheters we studied a multiobjective optimisation. The spectrum of solutions from a representative set of 100 non-dominated solutions is shown in Figure 20 for the PTV and the urethra for two monoenergetic point sources with photons energy of 20 and 40 keV.

Figure 21 shows the V_{150} and D_{90} range for the PTV and the D_{10} range for the urethra. The spectrum of solutions from a representative set of 100 non-dominated solutions is shown in Figure 21 for the PTV and the urethra for ^{192}Ir and a monoenergetic point source with photon energy of 100 keV.

The results demonstrate that optimisation results can differ and some solutions which can be obtained by one source type are not available from other types of sources. The results show that the characteristic properties of the sources are important.

Multiobjective dose optimisation is important in order to obtain a better understanding of the limitations and possibilities of dose optimisation in brachytherapy. Taking only a single solution by a single objective dose optimisation algorithm would not give this information.

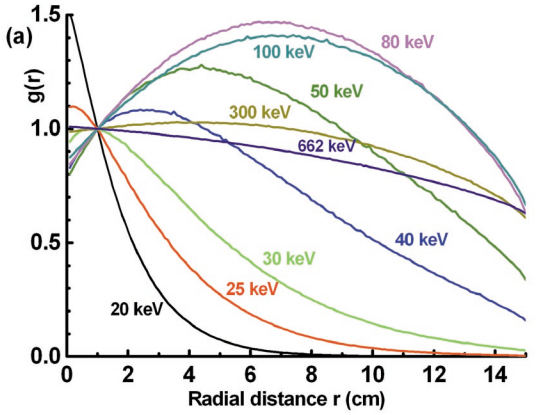

Figure 19a

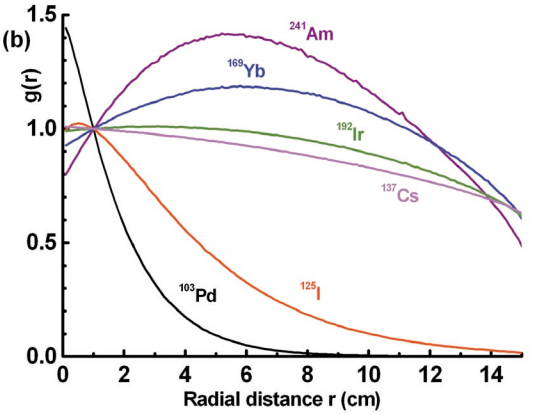

Figure 19b

Figure 19. Radial dose function g(r) for points sources (a) for various photon energies and (b) for various isotopes

The dose distributions that can be obtained depend not only on the position of the sources or SDPs but also

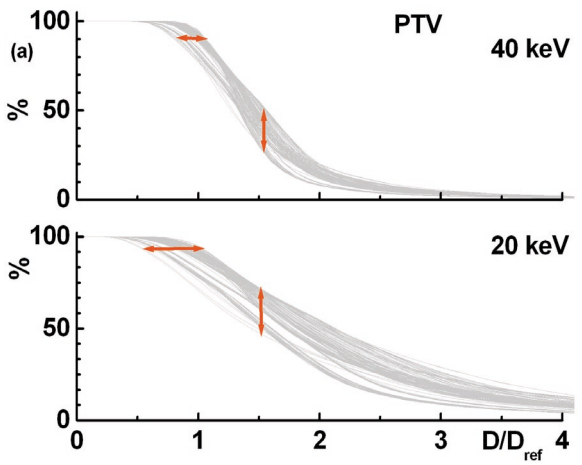

Figure 20a

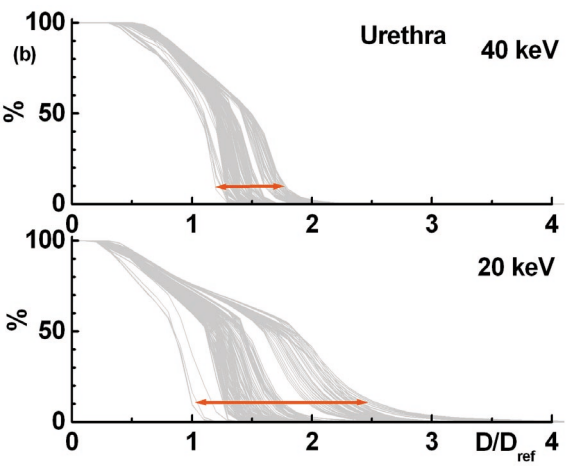

Figure 20b

Figure 20. Spectrum of DVHs for the PTV and the urethra for a prostate implant from solutions obtained by multiobjective dose optimisation for monoenergetic point sources with photon energy of 20 and 40 keV

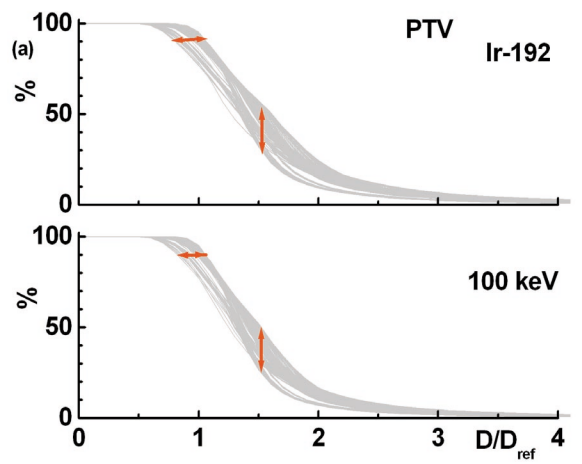

Figure 21a

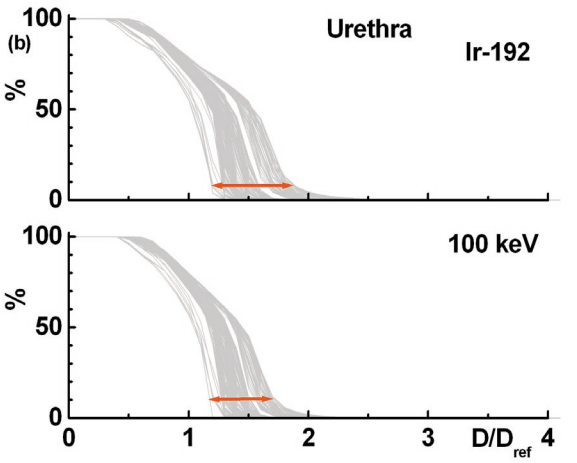

Figure 21b

Figure 21. Spectrum of DVHs for the PTV and the urethra for a prostate implant from solutions obtained by multiobjective dose optimisation for monoenergetic point sources with photon energy of 100 keV and for a ^{192}Ir source

on the energy spectrum. Considering this in inverse planning additional to the catheter geometry and the number of sources could lead to a *generalized multi-objective inverse planning* which can further improve the dose distributions that can be obtained.

Conclusions

Inverse planning in brachytherapy has entered a new era where previous empirical methods will be replaced by automatic computerized methods. The speed of current computers allows for the first time, users to obtain solutions adapted to the real anatomy of the tumour and the OARs. With multiobjective optimisation it is possible to obtain information that can be used to obtain the optimum number of catheters, their position and the optimum distribution of dwell times for HDR brachytherapy. For LDR brachytherapy also the stability of solutions due to seed migration can also be improved.

Treatment planners may require some time to abandon some of the methods they learnt to use and training and start to use inverse planning in the clinical routine. This is in part a philosophical problem because planners are not used to consider *inverse problems*.

With multiobjective optimisation a spectrum of alternative solutions is available and the treatment planner can select the solution that best satisfies the clinical constraints. All computer-based inverse planning methods provide better dose distributions that can be obtained by experienced planners.

More important than the gain of quality by multiobjective inverse planning is that the planners will recognize that empirical methods require a much larger time to obtain a satisfactory solution requiring adjustments of the catheter positions than the automatic adaptive inverse planning methods.

Tools have been developed for computer tomography [61] and recently 3D-ultrasound imaging based brachytherapy [62, 63] that allows the very fast automatic or semiautomatic accurate definition of the PTV and OARs together with a fast reconstruction of the catheters. Conformal anatomy-based dose optimisation allows the prescription of higher dose values and requires modern three-dimensional imaging-based brachytherapy.

This reduces the overall treatment time significantly allowing the treatment of more patients and reducing the cost implications. In 21st century medicine this is a very important factor and one which should not be ignored when developing new ideas.

Michael Lahanas, PhD
Department of Medical Physics & Engineering
Strahlenklinik
Klinikum Offenbach
Starkenburgring 66
63069 Offenbach am Main, Germany
e-mail: mlahanas@gmx.de

5 References

1. Groetsch CW. *Inverse Problems: Activities for Undergraduates*. The Mathematical Association of America; 1999.
2. Kirsch A. *An Introduction to the Mathematical Theory of Inverse Problems*. Springer, 1996.
3. Kolotas C, Birn G, Baltas D et al. guided interstitial high-dose rate brachytherapy for recurrent malignant gliomas. *Br J Radiol* 1999; 72: 805-8.
4. Kolotas C, Baltas D, Zamboglou N. CT-based interstitial HDR brachytherapy. *Strahlenther Onkol* 1999; 175: 419-27.
5. Zamboglou N, Kolotas C, Baltas C et al. Clinical evaluation of CT based software in treatment planning for interstitial HDR brachytherapy. In: *Brachytherapy for the 21st Century*, edited by B. L. Speiser and R. F. Mould. Nucletron B. V., The Netherlands, 1998, pp. 312-26.
6. Di Biase SJ, Hosseinzadeh K, Gullapalli RP et al. Magnetic resonance spectroscopic imaging-guided brachytherapy for localized prostate cancer. *Int J Radiat Oncol Biol Phys* 2002; 52: 429-38.
7. Kini VR, Edmundson GK, Frank MS et al. Use of three-dimensional radiation therapy planning tools and intraoperative ultrasound to evaluate high dose rate prostate brachytherapy implants. *Int J Radiat Oncol Biol Phys* 1999; 43: 571-8.
8. Tsalpatouros A, Baltas D, Kolotas C et al. CT based software for 3-D Localisation and Reconstruction in Stepping Source Brachytherapy. *IEEE Trans Inform Techni Biomed* 1997; 1: 229-42.
9. Milickovic N, Baltas D, Giannouli S et al. A new algorithm for autoreconstruction of catheters in computed tomography-based brachytherapy treatment planning. *IEEE on Biomedical Engineering* 2001; 48: 372-83
10. Milickovic N, Giannouli S, Baltas D, Lahanas M et al. Catheter autoreconstruction in computed tomography based brachytherapy treatment planning *Med Phys* 2000; 27: 1047-59.
11. Lahanas M, Baltas D, Zamboglou N. Anatomy-based three-dimensional dose optimization in brachytherapy using multiobjective genetic algorithms. *Med Phys*1999; 26: 1904-18.
12. Lahanas M, Baltas D, Zamboglou N. A hybrid evolutionary multiobjective algorithm for anatomy based dose optimisation algorithm in HDR brachytherapy. *Phys Med Biol* 2003; 48: 399-415.
13. Lessard E, Pouliot J. Inverse planning anatomy-based dose optimisation for HDR-brachytherapy of the prostate using fast simulated annealing and dedicated objective functions. *Med Phys* 2001;28:773-779.
14. Milickovic N, Lahanas M, Papagiannopoulou M et al. Multiobjective anatomy-based dose optimisation for HDR-brachytherapy with constraint free deterministic algorithms. *Phys Med Biol* 2002; 47: 2263-80.
15. Miettinen KM. *Nonlinear Multiobjective Optimisation*. Boston: Kluwer Academic Publisher; 1999.
16. Yu Y. Multiobjective decision theory for computational optimization in radiation therapy. *Med Phys* 1997; 24: 1445-54.
17. Schrijver A. *Linear and Integer Programming*. New York: Wiley; 1986.
18. Lee EK, Mitchell JE. *Branch-and-bound methods for integer programming, Encyclopedia of Optimization. CA Floudas and PM Pardalos* (ed.). Dordrecht: Kluwer; 1999.
19. Deb K and Agrawal R B. Simulated binary crossover for continuous search space. *Complex Systems* 1995; 9: 115-48.
20. Deb K and Goyal M. A combined genetic adaptive search (GeneAS) for engineering design. *Computer Science and Informatics* 1996; 26: 30-45.
21. Michalewicz Z. *Genetic Algorithms + Data Structures = Evolution Programs*. Springer Verlag; 1996.
22. Meyer S, Schweidler E. *Radioaktivität*. Berlin: Teubner; 1916, 70-6.
23. Sievert R. Die Intensitätsverteilung der primären gamma Strahlung in der Nähe medizinischer Radiumpräparate. *Acta Radiologica* 1921; 1:89.
24. Mould RF. *A century of X-rays and radioactivity in medicine with emphasis on photographic records of the early years*. Bristol & Philadelphia: Institute of Physics Publishing; 1993.
25. Mayneord WV. The distribution of radiation around simple radioactive sources. *Brit J Radiology* 1932; 5: 677.
26. Meredith WJ (ed). *Radium dosage. The Manchester system*. 2nd. edn. Edinburgh: Livingstone; 1947.
27. Godden TJ. *Physical aspects of brachytherapy*. Bristol: Adam Hilger; 1988.
28. Sievert R. Eine methode zur messung von Röntgen, Radium und Ultrastrahlung nebst einige untersuchungen über die anwendbarkeit derselben in der physik und der Medizin. *Acta Radiologica*, Supplementum 14; 1932.
29. Mould RF. *The calculation of the distribution of absorbed energy from gamma ray sources in media of low atomic number*. MSc dissertation, University of London, 1966.
30. Young MEJ, Batho HP. Dose tables for linear radium sources calculated by an electronic computer. *Brit J Radiology* 1964; 37, 38 & 689.

31. Paterson R and Parker HM. A dosage system for gamma-ray therapy. *Brit J Radiology* 1934; 7: 592.
32. Paterson R, Parker HM, Spiers FW. A system of dosage for cylindrical distributions of radium. *Brit J Radiology* 1936: 9: 487.
33. Paterson R and Parker HM. A dosage system for interstitial radium therapy. *Brit J Radiology* 1938; 11: 252 and 313.
34. Tod M, Meredith WJ. A dosage system for use in the treatment of cancer of the uterine cervix. *Brit J Radiology* 1938; 11: 809.
35. Hilaris BS, Nori D, Anderson LL. *Atlas of brachytherapy*. New York: Macmillan; 1988.
36. Kneschaurek P, Wehrmann R. Optimization of activity distribution in brachytherapy. *Med Phys* 1987; 14: 602-7.
37. Xio-Hong W, Potters L. A theoretical derivation of the nomograms for permanent prostate brachytherapy. *Med Phys* 2001; 29: 683-7.
38. Davison B. Distributions, in a non-absorbing body, of gamma-ray sources giving a uniform distribution of gamma rays. In: Mayneord W. V. 1950 Some applications of nuclear physics applied to medicine. *Br J Radiol*, Suppl. no 2 appendix III pp. 197-198.
39. Mayneord WV. Some applications of nuclear physics to medicine. *Br J Radiol* Suppl. no 2, Production of uniform field of radiation in a sphere 1950 p.150.
40. Meredith WJ. Personal communication R.F. Mould, 1979.
41. Murdoch J. Dosage in radium therapy. *Brit J Radiology* 1931; 4: 256.
42. Alfredo R, Siochi C, Elson HR et al. A self-collimating convolution backprojection algorithm for optimizing dose distributions of I-125 prostate implants *Med Phys* 1997; 24: 241-9.
43. Mayneord WV. Energy absorption. *Br J Radiol* 1940; 13: 235.
44. Mayneord WV. The measurement of radiation for medical purposes. *Proc Phys Soc* 1942; 54: 405.
45. Johns HE, Cunningham JR (eds). *The Physics of Radiology*. 3rd edn. Springfield: Charles C Thomas; 1969 pp 411-2.
46. Yu Y, Anderson LL, Li Z et al. Permanent prostate seed implant brachytherapy: Report of the American Association of Physicists in Medicine Task Group No. 64. *Med Phys* 1999; 26: 2054-76.
47. Butler WM, Merrick GS, Lief JH et al. Comparison of seed loading approaches in prostate brachytherapy. *Med Phys* 2000; 27: 381-92.
48. Chen Y, Stanton R, Holst R et al. Treatment planning for prostate implant with loose seeds. *Med Phys* 1997; 24: 1141-5.
49. Sloboda R. Optimization of brachytherapy dose distributions by simulated annealing. *Med Phys* 1992; 19: 955-64.
50. Sloboda R, Pearcy RG, Gillan SJ. Optimized low dose rate pellet configurations for intravaginal brachytherapy. *Int J Radiat Oncol Biol Phys* 1993; 26: 499-511.
51. Pouliot J, Tremblay D, Roy J et al. Optimization of Permanent 125I Prostate Implants using Fast Simulated Annealing. *Int J Radiat Oncol Biol Phys* 1996; 36: 711-20.
52. Guozhen Y, Reinstein LE, Pai S et al. A new genetic algorithm technique in optimization of permanent 125I prostate implants. *Med Phys* 1998; 25: 2308-15.
53. Yu Y, Schell MC. A genetic algorithm for the optimization of prostate implants. *Med Phys* 1996; 23: 2085-91.
54. Yu Y, Zhang JBY, Brasacchio RA, et al. Automated treatment planning engine for prostate seed implant brachytherapy. *Int J Radiat Oncol Biol Phys* 1999; 43: 647-52.
55. Lee EK, Gallagher RJ, Silvern D et al. Treatment planning for brachytherapy: an integer programming model, two computational approaches and experiments with permanent prostate implant planning. *Phys Med Biol* 1999; 44: 145-65.
56. D'Souza WD, Meyer RR, Thomadsen BR et al. An iterative sequential mixed-integer approach to automated prostate brachytherapy treatment plan optimization. *Phys Med Biol* 2001; 46: 297-22.
57. Edmundson GK, Yan D, Martinez AA. Intraoperative optimisation of needle placement and dwell times for conformal prostate brachytherapy. *Int J Radiat Oncol Biol Phys* 1995; 33: 1257-63.
58. Gandibleaux X, Morita H, Katoh N. The Supported Solutions Used as a Genetic Information in Population Heuristic, in Proceedings of the first international conference, EMO 2001, Zurich, Switzerland, edited by E. Zitzler, K. Deb, L. Thiele, C. A. Coello Coello, D. Corne, Lecture Notes in Computer Science Vol. 1993, Springer; 2001 429-442.
59. Milickovic N, Lahanas M, Baltas D et al. Comparison of Evolutionary and Deterministic Multiobjective Algorithms for Dose Optimisation in Brachytherapy, in Proceedings of the first international conference, EMO 2001, Zurich, Switzerland, edited by E. Zitzler, K. Deb, L. Thiele, C. A. Coello Coello, D. Corne, Lecture Notes in Computer Science Vol. 1993, Springer; 2001 167-180.
60. Cha C, Potter L, Ashley R et al. Isotope selection for patients undergoing prostate brachytherapy. *Int J Radiat Oncol Biol Phys* 1999; 45: 391-5.
61. Baltas D, Milickovic N, Giannouli S et al. New Tools of Brachytherapy Based on Three-Dimensional Imaging. *Front Radiat Ther Oncol* Basel. Karger Vol. 2000; 34: 59-70.
62. Straßmann G, Kolotas C, Heyd R et al. Navigation System for Interstitial Brachytherapy. *Radiotherapy and Oncology* 2000; 56:49-57.
63. Fenster A, Downey DB, Cardinal HN. Three-dimensional ultrasound imaging. *Phys Med Biol* 2001; 46: 67-99.

Paper received and accepted: 28 July 2003